ResearchGate

See discussions, stats, and author profiles for this publication at:
https://www.researchgate.net/publication/298215308

Imaging collective cell migration and hair cell regeneration in the sensory lateral line

Chapter · February 2016

DOI: 10.1016/bs.mcb.2016.01.004

READS

35

4 authors, including:



Andres Romero-Carvajal

Pontifical Catholic University of Ecuador

7 PUBLICATIONS **67** CITATIONS

SEE PROFILE



Tatjana Piotrowski

Stowers Institute for Medical Research

34 PUBLICATIONS **1,612** CITATIONS

SEE PROFILE

All in-text references underlined in blue are linked to publications on ResearchGate, letting you access and read them immediately.

Available from: Marina Venero Galanternik
Retrieved on: 22 May 2016

Imaging collective cell migration and hair cell regeneration in the sensory lateral line

M. Venero Galanternik
Stowers Institute for Medical Research, Kansas City, MO, United States
University of Utah, Salt Lake City, UT, United States
J. Navajas Acedo
Stowers Institute for Medical Research, Kansas City, MO, United States
A. Romero-Carvajal*, T. Piotrowski[1]
Stowers Institute for Medical Research, Kansas City, MO, United States
University of Utah, Salt Lake City, UT, United States
Current address: Pontificia Universidad Católica del Ecuador, Quito, Ecuador
[1]*Corresponding author: E-mail: pio@stowers.org*

CHAPTER OUTLINE

Introduction **3**
1. Lateral Line Development **3**
2. In Vivo Imaging of Lateral Line Primordium Migration **6**
2.1 Transgenic Lines 7
2.2 Anesthetizing the Embryos 7
2.2.1 Untreated embryos 7
2.2.2 Treated embryos 13
2.3 Embryo Mounting for Imaging 13
2.4 Confocal Time-Lapse Imaging of the Lateral Line Primordium 15
2.5 Post Time-Lapse Analysis 18
2.5.1 When embryos are kept alive 18
2.5.2 When embryos are fixed (for in situ hybridization, immunohistochemistry, etc.) 18
3. Live Labeling of Lateral Line Cells **18**
3.1 Labeling Lateral Line With Vital Dyes 23
3.1.1 BODIPY 505/515 and BODIPY-ceramide staining 23
3.1.2 DASPEI and FM lipophilic dyes 23
3.2 Cell Lineage Tracing and Clonal Analysis Behavior 24
3.2.1 Transplantations 24

Methods in Cell Biology, Volume 133, ISSN 0091-679X, http://dx.doi.org/10.1016/bs.mcb.2016.01.004
© 2016 Elsevier Inc. All rights reserved.

3.2.2 mRNA and DNA microinjections 25
3.2.3 Photoconvertible fluorescent proteins 25
4. Nonvital Tissue Labeling of Lateral Line Cells 26
4.1 Nuclear Labeling with 4′,6-Diamidino-2-Phenylindole 26
4.2 Alkaline Phosphatase Staining 27
4.3 Phalloidin Staining 27
5. Interpretation of Common Phenotypes 28
6. Hair Cell Regeneration 29
7. Long-Term Time-Lapse Analyses of Regenerating Neuromasts 29
7.1 Immobilization 30
7.2 Hair Cell Death 30
7.3 Time-Lapse Analysis and Tracking of Support Cells During Regeneration 31
7.3.1 Spatial sampling (setting up the Z-stack) 31
7.3.2 Recording time and time sampling 32
7.3.3 Suggested parameters for time-lapse recordings of regenerating neuromasts 32
7.4 Image Processing and Lineage Tracking 32
7.5 Cell Movement Analysis 34
7.5.1 Parameters 34
7.6 Spatial Analysis of the Origin of Support and Hair Cell Progenitors in Fixed Larvae 35
7.7 BrdU Incorporation 36
7.8 Immunohistochemistry 36
7.9 Data Acquisition, Processing, and Analysis 37
7.10 Statistical Analyses of Spatial Distribution 38
7.10.1 Quadrant analysis 38
7.10.2 Distance from center analysis 38
Conclusions 38
Acknowledgments 38
References 39

Abstract

The accessibility of the lateral line system and its amenability to long-term in vivo imaging transformed the developing lateral line into a powerful model system to study fundamental morphogenetic events, such as guided migration, proliferation, cell shape changes, organ formation, organ deposition, cell specification and differentiation. In addition, the lateral line is not only amenable to live imaging during migration stages but also during postembryonic events such as sensory organ tissue homeostasis and regeneration. The robust regenerative capabilities of the mature, mechanosensory lateral line hair cells, which are homologous to inner ear hair cells and the ease with which they can be imaged, have brought zebrafish into the spotlight as a model to develop tools to treat human deafness. In this chapter, we describe protocols for long-term in vivo confocal imaging of the developing and regenerating lateral line.

INTRODUCTION

Due to their transparency, zebrafish are an excellent model system to study morphogenetic cell behaviors, such as collective cell migration during development and regeneration in mature animals in vivo (Kimmel, Ballard, Kimmel, Ullmann, & Schilling, 1995). The developing and regenerating sensory lateral line system has been an especially powerful model system to study cell behaviors in vivo due to its accessibility and amenability to genetic or chemical manipulations (Chen, Harris, Levesque, Nusslein-Volhard, & Sonawane, 2012; Diotel et al., 2011; Kimmel et al., 1995). The lateral line is a mechanosensory system that enables aquatic vertebrates to sense water motion and orient themselves in their environment. The lateral line system consists of mechanosensory organs in the skin called neuromasts that are arranged in lines around the eye, on the lower jaw, and on the trunk (Aman & Piotrowski, 2010; Dambly-Chaudiere et al., 2003; Metcalfe, 1985). Lateral line sense organs perceive low-frequency oscillations, discriminate the source, and provide information about distance, hence playing an important behavioral role in prey–predator interactions, feeding, navigation, schooling, and mating (Sienknecht, Koppl, & Fritzsch, 2014). Each neuromast is volcano-shaped and consists of a central group of hair cells surrounded by support cells and an outer ring of mantle cells (Fig. 1A and B) (Ghysen & Dambly-Chaudiere, 2004, 2007; Lush & Piotrowski, 2014b). The mechanosensing hair cells in the lateral line are homologous to the hair cells in the mammalian inner ear that transduce vibrations caused by sound waves and develop by very similar mechanisms (Fritzsch & Straka, 2014).

1. LATERAL LINE DEVELOPMENT

Even though zebrafish possess an anterior and a posterior lateral line, most studies have focused on the posterior lateral line, because of the ease with which it can be imaged (Fig. 2A). The zebrafish posterior lateral line develops from an ectodermally derived thickening known as the lateral line placode or primordium (Dambly-Chaudiere et al., 2003; Ghysen & Dambly-Chaudiere, 2004; Piotrowski & Baker, 2014). This placode, which is comprised of approximately 100 cells, delaminates posterior to the otic vesicle at around 18–20 hours postfertilization (hpf) and segregates into a nonmigrating lateral line ganglion, and the migratory lateral line primordium (Fig. 2B) (Dambly-Chaudiere et al., 2003; Kimmel et al., 1995; Metcalfe, Kimmel, & Schabtach, 1985). At 22 hpf, the primordium begins its migration within the epidermis and along the horizontal myoseptum toward the tail tip (Chitnis, Nogare, & Matsuda, 2012; Ghysen & Dambly-Chaudiere, 2007; Metcalfe, 1985). A particular striking cellular process is the periodic deposition of protoneuromasts by the primordium as it migrates (Fig. 2C). After deposition, these protoneuromasts differentiate into mature neuromasts that are comprised of centrally located hair cells surrounded by support cells. The support cells are in turn surrounded by a ring of mantle cells (Fig. 1A–D, F). At the end of migration, at approximately

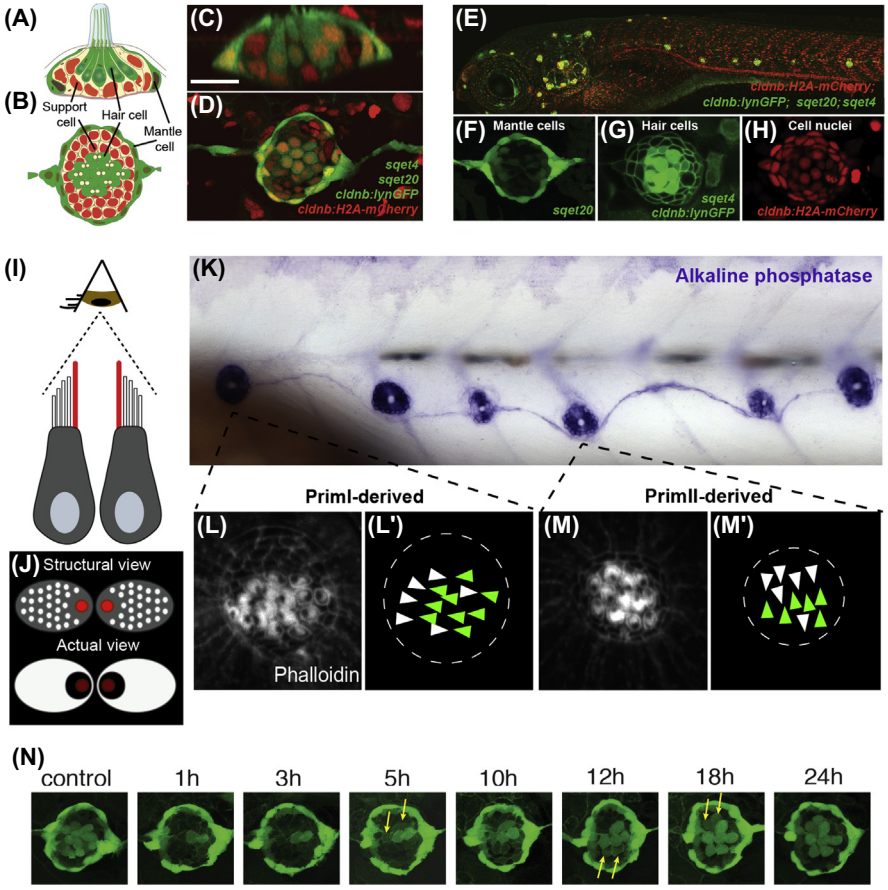


FIGURE 1 Morphology of the sensory lateral line system.

(A) Horizontal and (B) lateral views of a schematic neuromast. White spots in the central hair cells depict the localization of the kinocilia. (C–H) Quadruple transgenic larvae express the mantle cell marker *sqet20* (F, green (gray in print versions)), the hair cell marker *sqet4* (G, cytoplasmic green (gray in print versions)), the cell membrane marker *cldnb:lynGFP* (G), and the nuclear maker *cldnb:H2A-mCherry* (H, red (dark gray in print versions)) *(Modified after Romero-Carvajal, A., Navajas Acedo, J., Jiang, L., Kozlovskaja-Gumbriene, A., Alexander, R., Li, H., & Piotrowski, T. (2015). Regeneration of sensory hair cells requires localized interactions between the Notch and Wnt pathways. Developmental Cell, 34, 267–282).* (I–J) Schematic of dorsal view of a pair of mirror-polarized hair cells. The absence of Phalloidin staining reveals at which pole of the cuticular plate the microtubule-based kinocilium is localized. (K) Alkaline phosphatase staining of primI- and primII-derived neuromasts. (L–L′, M–M′) PrimI- and primII-derived neuromasts possess hair cell polarities that are off set by 90°. *White and green arrows* (gray in print versions) depict hair cells with the same polarity, respectively. (N) Still images of a *Tg(sqET20;sqET4)* larval neuromast in the process of neomycin-induced regeneration. All hair cells, except two immature hair cells, were killed by neomycin at 1 h post neomycin. Two newly formed hair cells (*arrows*) start to express GFP at 5 h, and other pairs of hair cells (*arrows*) appear at 10 and 18 h.

Modified after Jiang, L., Romero-Carvajal, A., Haug, J. S., Seidel, C. W., & Piotrowski, T. (2014). Gene-expression analysis of hair cell regeneration in the zebrafish lateral line. Proceedings of the National Academy of Sciences of the United States of America, 111, *E1383–E1392.*

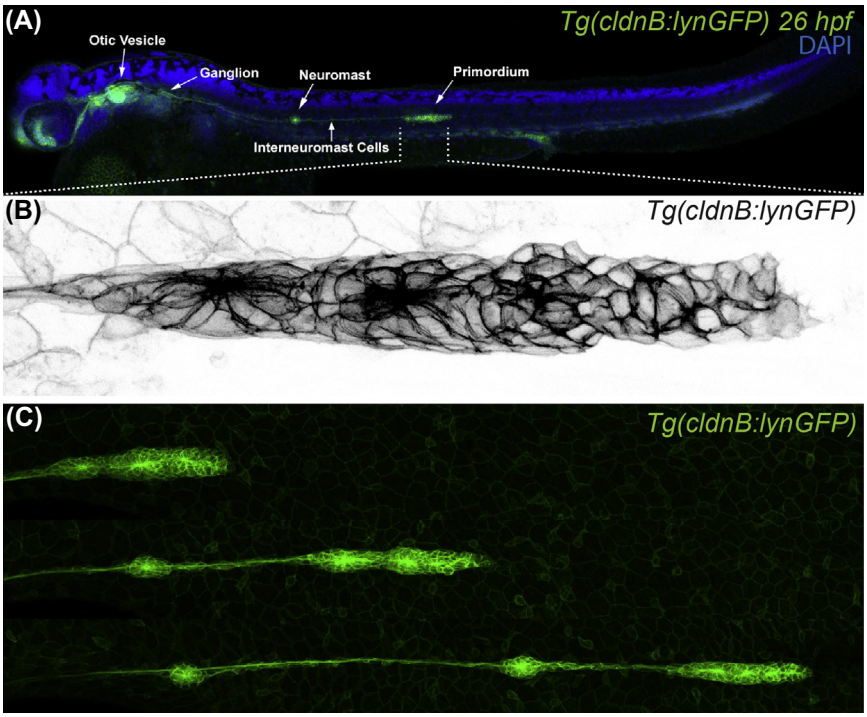


FIGURE 2 Still images of migrating primordia.

(A) Low magnification image of a 32 hpf *Tg(cldnb:lynGFP)* embryo in which the primordium has reached the middle of the trunk. (B) Magnification of a posterior lateral line primordium *(modified after Venero Galanternik, M., Kramer, K. L., and Piotrowski, T. (2015). Heparan sulfate proteoglycans regulate Fgf signaling and cell polarity during collective cell migration. Cell Reports, 10).* The leading region consists of mesenchymal cells, whereas protoneuromasts form in the trailing region. Protoneuromasts are detectable by central accumulation of ClaudinB:GFP. (C) Different stages of primordium migration illustrating the sequential deposition of protoneuromasts.

48 hpf, the migrating primordium has deposited five to six sensory neuromasts along the trunk. Once the primordium has reached the tail, it fragments and differentiates into two to three terminal neuromasts (Aman, Nguyen, & Piotrowski, 2011). At approximately 48 hpf a second primordium (primII) starts to migrate from posterior to the ear to the tail (Dambly-Chaudiere et al., 2003; Ghysen & Dambly-Chaudiere, 2007). It migrates considerably more slowly than primI and deposits a few neuromasts in between the primI-derived neuromasts (Fig. 1K).

The formation of garlic bulb-shaped protoneuromasts (also called rosettes) within the trailing 2/3 of the migrating primordium can be distinguished by a central region of apical constrictions (Lecaudey, Cakan-Akdogan, Norton, & Gilmour, 2008; Nechiporuk & Raible, 2008). Typically, two to three protoneuromasts can

be observed within a primordium (Fig. 2B) (Aman et al., 2011). Even though hair cells only fully differentiate once deposited, they are specified within protoneuromasts within the migrating primordium and can be distinguished by the expression of genes, such as *atoh1a*. In contrast, the leading 1/3 of the primordium does not show any signs of differentiation and the cells possess a mesenchymal morphology (Aman & Piotrowski, 2008; Ghysen & Dambly-Chaudiere, 2007). The identity of these morphologically distinct regions is determined by a regulatory feedback between Wnt/β-catenin signaling in the leading region and Fgf signaling in the trailing region of the primordium (Aman & Piotrowski, 2008; Chitnis et al., 2012; Thomas, Cruz, Hailey, & Raible, 2015).

While migration progresses, the primordium does not only deposit neuromasts but also leaves behind a chain of interneuromast cells in between that represent a latent pool of stem cells that postembryonically form additional neuromasts (Fig. 2A) (Ghysen & Dambly-Chaudiere, 2004; Grant, Raible, & Piotrowski, 2005; Lopez-Schier & Hudspeth, 2006; Lush & Piotrowski, 2014a). The timing of novel neuromast generation by interneuromast cells is regulated by glial cells that ensheath the neighboring lateral line axons (Goodrich, 2005; Lyons et al., 2005). Lateral line axons extend from the lateral line ganglion, follow the primordium as it migrates and innervate the sensory hair cells within each neuromast (Faucherre, Pujol-Marti, Kawakami, & Lopez-Schier, 2009; Gilmour, Knaut, Maischein, & Nusslein-Volhard, 2004; Metcalfe, 1985; Metcalfe et al., 1985; Shoji, Yee, & Kuwada, 1998). After neuromast deposition, hair cells are added via support cell proliferation and by 5 days postfertilization (dpf) mature neuromasts possess 12−15 hair cells. Subsequently, dividing and differentiating support cells replace randomly dying hair cells (Lush & Piotrowski, 2014b). Interestingly, in primI-derived neuromasts, hair cells are polarized along the anterior−posterior (A-P) axis of the embryo, whereas primII-derived neuromasts are polarized along the dorsoventral (D-V) axis (Lopez-Schier, Starr, Kappler, Kollmar, & Hudspeth, 2004). These different polarities allow the animal to sense water motion coming from different directions. It is not well understood how these polarities are established (Lopez-Schier et al., 2004).

Several imaging protocols tailored for long-term time lapse recordings of specific developing tissues and developmental stages are available (Distel & Koster, 2007, Kamei & Weinstein, 2005; Kaufmann et al., 2012; Renaud et al., 2011). In this chapter, we will describe detailed techniques for imaging and assessing posterior lateral line primordium migration from the ear to the tail in live and fixed embryos, as well as postmigratory events such as the formation of new neuromasts from interneuromast cells and hair cell regeneration.

2. IN VIVO IMAGING OF LATERAL LINE PRIMORDIUM MIGRATION

The analyses of primordium migration and hair cell regeneration are greatly facilitated by the availability of transgenic lines and markers that label all lateral line cells

or only subpopulations (Table 1). For example, lines that label the entire lateral line can be used to detect changes in proper lateral line morphogenesis caused by genetic or chemical perturbations (Table 2). Defects could occur in primordium migration speed, protoneuromast formation or deposition, or they could cause primordium stalling before it reaches the tail tip.

2.1 TRANSGENIC LINES

Zebrafish research has greatly benefited from the relative ease with which transgenic lines can be generated that express fluorescent markers in specific tissues of interest, facilitating live imaging. Lines that label the primordium, the lateral line axons, and/or neuromasts are described in Table 1. *Tg(cldnb:lynGFP)* is one of the most commonly used lines in lateral line studies (Haas & Gilmour, 2006). ClaudinB, a tight junction protein, is expressed strongly in tissues that originate from sensory placodes and labels all cell types of the developing lateral line (Kollmar, Nakamura, Kappler, & Hudspeth, 2001; Lopez-Schier et al., 2004).

Once a particular transgenic line has been selected, proceed with the following protocol for live imaging of the developing lateral line.

2.2 ANESTHETIZING THE EMBRYOS

We describe the protocols for untreated and manipulated wild-type, mutant, or transgenic embryos. For this procedure you will need:

- Tricaine (MS-222- 4 g/L pH 9.0)—1–5 mL (aliquots should be kept at −20°C)
- 100 mm Petri dish containing ~30 mL of 0.5X E2 medium
- Fire-polished glass Pasteur pipette
- Sorted and dechorionated embryos
- Straight stainless steel forceps #5 or #55

2.2.1 Untreated embryos

Once embryos are dechorionated, they need to be immobilized to ensure they are completely still during the imaging process. To achieve this, begin by adding 500–700 μL of Tricaine solution to 30 mL of 0.5X E2 in a 100 mm Petri dish, swirl gently, and let the embryos rest for 5 min.

Confirm that the embryos' hearts are beating and that the embryos are completely anesthetized by gently touching their tail or head with a pair of forceps. If the embryos respond by twitching, add another 50 μL of Tricaine and repeat the same process until the embryos are completely immobilized but the heart still firmly beats.

It is important to be patient during this procedure as a Tricaine overdose leads to embryo death when added in excessive amounts or too quickly. On the other hand, failure to attain complete immobilization will result in twitching of the embryo during image acquisition. In general, it is preferred to underanesthetize the embryo, as

Table 1 Transgenic Lines Commonly Used for Live Imaging of Lateral Line Migration and Hair Cell Regeneration

Transgenic Line	Expression Pattern	References
Tg(cldnb:lynGFP)^{zf106}	All lateral line cells	Haas and Gilmour (2006)
Tg(cldnb:H2A-mcherry)^{psi4}	All lateral line cell nuclei	Lush and Piotrowski (2014a, 2014b)
Tg(atp2b1a-GFP)^{sqET4}	Hair cells	Parinov, Kondrichin, Korzh, and Emelyanov (2004)
Tg(pou4f3:GAP-GFP)^{s356t}	Hair cells	Xiao, Roeser, Staub, and Baier (2005)
Tg(atoh1a:dTomato)^{nns8Tg}	Newly formed hair cells	Wada et al. (2010)
Tg(myo6b:mcherry^{CAAX})^{ru1002Tg}	mCherry in hair cell membranes	Mirkovic et al. (2012)
Tg(sox2-2a-sfGFP)^{stl84}	CRISPR-mediated insertion. *sox2* reporter in neuromast support cells	Shin, Chen, and Solnica-Krezel (2014)
TgBAC(cdh2:Cdh2-GFP)	Cadherin 2 reporter line	Revenu et al. (2014)
Et(krt4:EGFP)^{sET20}	Support and interneuromast cells	Parinov et al. (2004)
Tg(Tp1bglob:eGFP)^{um13} and Tg(T2KTp1bglob:hmgb1-mCherry)^{jh11}	Notch reporters in central support cells	Parsons et al. (2009)
Tg(−4.7alpl:mCherry)	Mantle cells	Steiner, Kim, Cabot, and Hudspeth (2014)
Tg(sdf1a:sdf1a-EGFP)^{p10}	BAC transgenic, chemokine ligand Cxcl12a reporter	Venkiteswaran et al. (2013)
Tg(cxcr4b:cxcr4b-Kate2-IRES-EGFP-CaaX)^{p7}	Cxcl12 (Sdf1a) signaling sensor	Venkiteswaran et al. (2013)
Tg(cxcr4b:cxcr4b-EGFP-IRES-Kate2-CaaX)^{p7}	Cxcl12 (Sdf1a) signaling sensor	Venkiteswaran et al. (2013)
Tg(tubb2b:cxcr7b-IRES-CFP-CaaX)^{p3}	Misexpresses the chemokine receptor Cxcr7b only in lateral line axons	Venkiteswaran et al. (2013)
TgBAC(cxcr4b:cxcr4b:NLS-Tomato)^{zf511Tg}	Nuclear localized Cxcr4b BAC reporter	Dona et al. (2013)
TgBAC(cxcr4b:cxcr4b-TagRFP-sfGFP,crybb1:ECFP)^{zf512Tg}	Tandem fluorescent protein timer reporter that recapitulates Cxcr4b expression and allows quantification of Cxcr4b-dependent receptor turnover in vivo	Dona et al. (2013)

Tg(UAS:kaede)^{rk8} *x Tg(cldnb4.2:gal4)*^{nim11}	Photoconvertible Kaede expressed in ClaudinB-expressing cells	Breau et al. (2013) and Hatta et al. (2006)
Tg(elavl3:Kaede)^{rw0130a}	Kaede expression in neurons including the lateral line ganglion and axons	Sato, Takahoko, and Okamoto (2006)
Tg(-4.9sox10:egfp)^{ba2}	Neural crest-derived cells including Schwann cells along the lateral line nerve	Carney et al. (2006)
Tg(-7.2sox10:dnHsa.ERBB4-RFP,myl7:EGFP)^{psi3Tg}	Leads to extra neuromast formation by inhibiting ErbB signaling in lateral line Schwann cells	Lush and Piotrowski (2014a, 2014b)
Tg(foxd3:gfp)^{zf15}	Schwann cells	Gilmour, Maischein, and Nusslein-Volhard (2002)
Tg(nerve:mem-GFP)	Lateral line nerve	Dona et al. (2013)
cntnap2a^{nkhgn39dET}	Lateral line ganglion and axons	Nagayoshi et al. (2008)
Tg(OTM:d2EGFP)^{kyu1}	Wnt/β-catenin-expressing cells in the primordium	Shimizu, Kawakami, and Ishitani (2012)
Tg(ubi:Zebrabow-M^{a131}*)*	Ubiquitous	Pan et al. (2013)

Table 2 Lateral Line Phenotypes

Manipulation Type	Mutant Line	Pathways Affected	Primordium Phenotype	References
Mutants	*apc*^{mcr}	Wnt/β-catenin	Primordium stalling due to Wnt/β-catenin expansion that results in *cxcr7b* inhibition.	Aman and Piotrowski (2008)
	lef1^{nl2} *and lef1*^{u767}		Incomplete migration due to reduced Wnt/β-catenin.	McGraw et al. (2011) and Valdivia et al. (2011)
	kremen^{nl10}		Incomplete primordium migration and dispersion of primordium cells into a single line of cells due to decreased Wnt/β-catenin signaling.	McGraw et al. (2014)
	odysseus/cxcr4b^{uIO049} *cxcr7b*^{sa16} *medusa/cxcl12a*^{t30516}	Chemokine	Primordium stalling.	Dona et al. (2013), Haas and Gilmour (2006), Valentin, Haas, and Gilmour (2007), and Venkiteswaran et al. (2013)
	dackel/ext2^{to79e} *boxer/extl3*^{tm70g}	Fgf	Primordium stalling due to Fgf signaling downregulation, resulting in Wnt/β-catenin expansion and *cxcr7b* inhibition.	Venero Galanternik et al. (2015)
	limabsent(lia)/fgf3^{t24149}; *daedalus(dae)/fgf10a*^{tbvbo}		Primordium stalling and loss of rosette formation in the double mutants. Partial phenotypes in the single mutants.	Lecaudey et al. (2008), Nechiporuk and Raible (2008), and Norton, Ledin, Grandel, and Neumann (2005)
	rowgain/erbb2^{t823}, *hypersensitive/erb3bb*^{tc288D,t5419}, *neuregulin1-3*^{z26}	ErbB	Extra neuromast formation due to lack of Schwann cells or lateral line axons.	Lush and Piotrowski (2014a, 2014b) and Lyons et al. (2005)
	colorless/sox10^{tw11,t3}			Grant et al. (2005)

	neurogenin1^{hi1059}		Extra neuromast formation due to lack of peripheral glia.	Lopez-Schier and Hudspeth (2005)
	mindbomb (*mib*^{ta52b},*mib*^{m178}, *mib*^{m132})	Notch	Primordium and neuromast fragmentation and stalling.	Itoh et al. (2003) and Matsuda and Chitnis (2010)
	amotl2a^{fu45} *amotl2a*^{fu46}	Hippo	Bigger primordium and more deposited neuromasts due to increased proliferation and upregulation of Wnt/β-catenin.	Agarwala et al. (2015)
	yap1^{fu47} *yap1*^{fu48}		Smaller and rounded primordium due to decreased proliferation.	
	tgfβ1a^{td5}	TGFβ/Smad5	Reduced number of deposited neuromasts and hair cells and increase of interneuromast distance.	Xing et al. (2015)
	glass onion/n-cadherin^{m117}	Cadherin junctions	Lateral line axon pathfinding defects suggest a primordium U-turning phenotype.	Kerstetter, Azodi, Marrs, and Liu (2004) and Malicki, Jo, and Pujic (2003)
	fused somites (fss)/tbx24^{te314}		Primordium U-turns and fails to migrate due to defects in chemokine ligand *cxcl12a* expression.	Haas and Gilmour (2006) and Nikaido et al. (2002)
	bap28/heatr1^{y75}	rRNA transcription and processing Apoptosis	Less deposited neuromast due to upregulated apoptosis[a]	Aman et al. (2011) and Azuma, Toyama, Laver, and Dawid (2006)
Chemical inhibition	SU5402 PD173074	Fgf	Primordium stalling due to Fgf signaling downregulation, resulting in Wnt/β-catenin expansion and *cxcr7b* inhibition.	Aman and Piotrowski (2008)
	Sodium chlorate ($NaClO_3$)	HSPGs/Fgf	Primordium stalling due to Fgf signaling downregulation, resulting in Wnt/β-catenin expansion and *cxcr7b* inhibition.	Venero Galanternik et al. (2015)

Continued

Table 2 Lateral Line Phenotypes—cont'd

Manipulation Type	Mutant Line	Pathways Affected	Primordium Phenotype	References
	BIO/AZK	Wnt/β-catenin	Complete stalling due to Wnt/β-catenin expansion that results in *cxcr7b* inhibition.	Lush and Piotrowski (2014a, 2014b) and Venero Galanternik et al. (2015)
	AG1478	ErbB	Formation of extra neuromasts due to loss of Schwann cells	Lush and Piotrowski (2014a, 2014b)
Transgenic lines	*Tg(hsp70:sdf1a)*	Chemokine	Primordium stalling due to overexpression of chemokine ligand *cxcl12a* without affecting signaling within the primordium.	Dona et al. (2013), Venero Galanternik et al. (2015), and Venkiteswaran et al. (2013)

[a] *Several morpholino-injected embryos will also recapitulate this phenotype in similar or more severe way. Interestingly most morpholinos tend to be extremely toxic to the lateral line cells and cause cell death that results in less deposited neuromasts or even the death of the primordium cells, however, when compared to their respective mutants these phenotypes do not always match each other (eg,* tcf7 *ATG morpholino vs* tcf7 *MZ mutants) (Aman et al., 2011).*

more Tricaine can be added to the E2 medium covering the mounted embryos right before the beginning of image acquisition.

2.2.2 Treated embryos

When drug-treated embryos are imaged, it is recommended to pretreat these embryos before mounting them in agarose. We would like to stress the importance of pilot in situ hybridization experiments to determine for how long embryos need to be pretreated before target genes are completely up- or downregulated. In our hands, at least 6 h of pretreatment are required. In the case of heat-shocked embryos, the assessment of how long the heat shock has an effect on gene expression is equally important.

Many commonly used pharmacological reagents are light sensitive (refer to individual product information sheets), including to different confocal laser wavelengths. Therefore, as described previously, one has to ensure that downstream targets are downregulated throughout the time lapse. To counteract the effects of drug degradation, the laser power can be kept lower or the drug solution can be exchanged several times.

To limit the amount of drug needed, 10−15 embryos are treated in 2 ml of solution. Once the treatment protocol has been established, begin by adding 25−50 μL of freshly thawed Tricaine solution to the embryos contained in 2 mL drug solution. Swirl gently and let the embryos rest for 5 min. Repeat as needed until the embryos are completely immobilized but the heart still beats firmly.

> *Note*: Pharmacological inhibitor activity varies extensively from lot to lot. Therefore, the titration of drug concentrations is important when determining an effective working concentration and should be performed every time a new drug is purchased.

2.3 EMBRYO MOUNTING FOR IMAGING

Embryo mounting for long-term lateral line migration recording is best achieved by embedding the embryos in 0.8% low melting point (LMP) agarose as it hardens more slowly than regular agarose, allowing the correct repositioning of the embryo for imaging (Fig. 3). LMP agarose will also allow the embryo tail to grow. For this procedure you will need:

- Anesthetized embryos in 0.5X E2 medium (7.5 mM NaCl, 0.25 mM KCl, 0.5 mM $MgSO_4$, 0.075 mM KH_2PO_4, 0.025 mM Na_2HPO_4, 0.5 mM $CaCl_2$, 0.35 mM $NaHCO_3$) with Tricaine (MS-222—4 g/L pH 9.0) or drug solution.
- 5 mL of LMP agarose (Promega—V3841) solution (0.8% in 0.5X E2 medium) stocks. If kept at 4°C, place tube in a beaker containing water and microwave for 1−2 min or until the agarose is completely dissolved.
- 35-mm MatTek glass bottom microwell dish (uncoated, 20-mm diameter microwell, N° 1.5 coverglass, 0.16−0.19 mm; P35G-1.5−20-C).
- 1.5-mL clear centrifuge tubes.
- Heat block at 43°C.

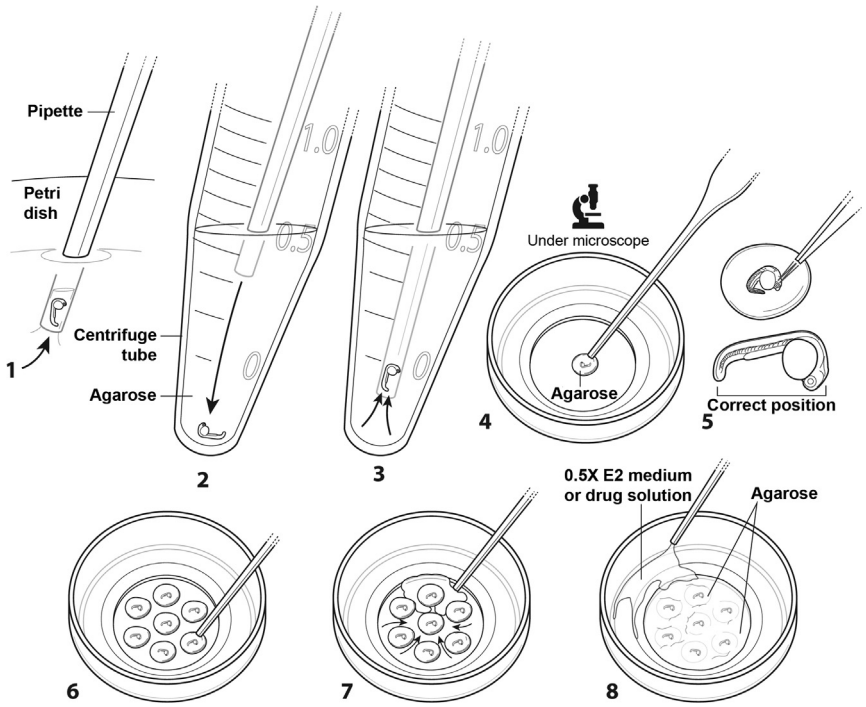


FIGURE 3 Schematic of how to mount embryos in low melting point agarose for long-term time-lapse analysis.

Each step is described in detailed in the in vivo imaging of lateral line primordium migration section.

- Fire-polished glass Pasteur pipette.
- A pair of stainless steel straight forceps #5 or #55.

1. Place the agarose solution in a heat block at 43°C and let the temperature equilibrate for 15 min before beginning the procedure. Subsequently, add 300 μL of 4 g/L Tricaine to the agarose.
2. Transfer 500 μL of agarose into a 1.5 mL tube with a fire-polished glass Pasteur pipette. Transfer one embryo from the dish into the tube with as little E2 medium as possible. To replace the water surrounding the embryo with agarose, let the embryo sink to the bottom of the tube and suck it back into the pipette together with some agarose.
3. Under a dissecting microscope place a ~5-mm diameter drop of agarose containing the embryo in the center of the MatTek dish. Use forceps to position the embryo with the lateral side of the embryos facing you (sideways) and as close to the bottom of the dish as possible.
4. To obtain a fairly flat mounted embryo, gently keep pushing the embryo by placing the forceps on its head, trying very carefully to not push or bend the tail.

Zebrafish tails are fairly stiff and therefore by moving the head, the trunk, and tail will orient themselves parallel to the bottom of the dish.

5. When an embryo is properly mounted, both eyes are parallel to each other (you can only see the eye closest to you) and all somites are in a single focal plane. Once the embryo is positioned in the desired orientation, keep the embryo in place with the forceps or reorient the embryo several times until the agarose has solidified (about 1 min).
6. Mount five to seven embryos in a MatTek dish, each in its individual drop of agarose. Mounting more than one embryo increases the chances of obtaining at least one well-mounted embryo, as not all the embryos will be totally flat.
7. Allow each drop of agarose to solidify for 3–5 min. Subsequently, fill the gaps in between each drop with a thin layer of agarose covering the entire glass bottom of the MatTek dish. Let the agarose solidify for 3–5 min.
8. Finally, add 2–3 mL of 0.5X E2 medium or drug solution containing Tricaine with a glass pipette. Add solution very slowly against the wall of the MatTek dish. Do not squirt the E2 medium directly onto the agarose as this can cause the embedded embryos to detach from the glass bottom. Place a lid on the MatTek dish to inhibit water evaporation during long time-lapse recordings and start imaging.

   Note: If the mounted embryos are going to be transported from one room to another, add the E2 medium only once you have reached the microscope room, as rough or sudden movements will lead to the detachment of the agarose from the glass bottom. Finally, if working with light sensitive drugs, keep light exposure to a minimum while mounting to reduce light-induced drug degradation and always use a freshly made drug solution before imaging.

2.4 CONFOCAL TIME-LAPSE IMAGING OF THE LATERAL LINE PRIMORDIUM

Primordium migration is best recorded on an inverted multiphoton confocal microscope. We have tested light sheet and spinning disc confocals and found that the resolution was lower. However, these scopes scan at a higher speed, reducing acquisition times considerably. If a confocal microscope is not available, time lapses can also be recorded on an automated, inverted/upright compound fluorescence microscope, but it is important to point out that while current compound microscopes do facilitate multiple plane imaging (Z-stack) with reasonable resolution and contrast, they usually are not suitable for thicker sample imaging (Jonkman & Brown, 2015). Therefore, single plane time-lapse acquisition is recommended to avoid high signal to noise and blurry time lapses.

Because the primordium travels for several micrometers along the entire length of the trunk, confocal microscopes that run with software that allows tiling are optimal. This feature enables the analysis of large areas by acquiring an overview of several aligned individual images (or tiles). Alternatively, if the software does not support tiling, the stage can be readjusted every few hours before the primordium

leaves the field of view and the individual movies can be later stitched in ImageJ (Plugins > Stitching > Deprecated > 3-D stitching).

The advantage of an inverted microscope is that the objective is closer to the sample and importantly, it allows mounting of embryos in a water-filled Petri dish with a lid. If only upright equipment is available, it is recommended to use immersion lenses for image acquisition; however, evaporation of the medium will be an issue.

Lateral line primordium migration can be observed with different magnifications (10−63X). A general migration assessment can be successfully achieved by imaging the primordium using a 10X objective. However, the best cellular resolution is obtained with a 40X (or higher) long-working distance objective (eg, Zeiss LD C-Apochromat 40X/1.1 water Korr M27). As the tail is not mounted flat against the coverslip, 40X or 63X objectives with standard working distances are not suitable.

Additionally, to allow the embryos to develop according to the normal table of zebrafish development (Kimmel et al., 1995), time-lapse recording should optimally be acquired in an incubation chamber or on heating stage set to 28.5°C. If an incubator is used, it is important to let the dish with the mounted embryos equilibrate for 30 min to avoid any focus drift from the warming agarose.

If you aim to record the entire primordium migration from ear to tail, start at 20−22 hpf. Recordings of earlier stages of lateral line development, such as placode formation that occurs close to the head region, are difficult to combine with recordings of migration along the trunk, as they occur in very different focal planes. To surpass this problem, shorter time lapses can be recorded of multiple smaller regions. These independent movies can later be stitched using ImageJ. Alternatively, using lower magnification (10−20X) will allow for complete migration acquisition starting at earlier stages (18−20 hpf), although at a lower cellular resolution. Unfortunately, because younger embryos (≤20 hpf) are still extending their tails, proper growth will be compromised.

- Time lapses are acquired in a 4-dimensional format (X, Y, Z, *t*):
  X-axis: length of image in micrometers—defined by the objective.
  Y-axis: height of image in micrometers—defined by the objective.
  Z-axis (Z-stack, range): depth in micrometers within the sample containing all optical slices (sections or planes). The Z-axis is established by selecting the top and bottom sections to be imaged correspond to the top and bottom sections that are closer or further away from the coverslip, respectively. The Z-axis length encompasses the optical slices, separated uniformly by a determined number of slice intervals (micrometers) that will not be imaged.
  Time (t): Sum of all Acquisition Cycles (total time required to obtain all Z-stacks (X + Y + Z) plus a designated time break before starting a new one).

1. Proceed to choose the most flatly mounted embryo, which will require the fewest number of Z-planes and shortest acquisition time (*t*), allowing a shorter time interval between Z-stacks resulting in a more detailed and smooth time lapse.

2. When setting up the Z-stack, ensure the skin is included, as the embryo will continue to grow, not only in the anterior−posterior orientation but it will also gain some volume.
3. Next, determine how many tiles are required to cover a desired region along the embryo trunk. A tile or single image comprises a determined area (X,Y), dictated by the magnification/objective employed for acquisition.

For example, if a single tile image covers an area of 100 μm (10 × 10 μm) using a 40X objective, and the final image is set up in a 5:1 tile configuration (contains five horizontal and one vertical tiles), each designated tile will be of this size as well, producing an image that covers a 500 μm area (50 × 10 μm).

4. To set up the tiling parameters focus on the midpoint of the primordium migration path, which is usually at the end of the yolk extension, as the software will move the stage using this area as the middle point for scanning each tile and it will represent the exact center of the acquired image.
5. At 40X magnification, choose a 5:1 (horizontal:vertical) tile conformation with 20% overlap for 24−48 hpf wild-type embryos. The third horizontal tile of the image should be the area at the end of the yolk extension.
6. The depth of the Z-stack will vary from embryo to embryo, however, when comparing a wild-type sample to an experimental embryo, it is recommended to use the same "Acquisition Cycle" times as this will facilitate direct comparison of parameters like:
   - Size comparison of the primordia, neuromasts, and interneuromast cells.
   - Primordia morphologies (leading and trailing regions).
   - Primordia speeds (migration speed, traversed distance, or somite number within a time frame).
   - Deposition rates (number of neuromasts deposited per distance traveled).
   - Cell behaviors (protrusions, directionalities).
7. Some suggested imaging parameters for acquiring lateral line Z-stacks at *40X magnification*:
   - Z-axis (Z): 15−50 μm.
   - Number of optical slices within a Z-stack: 5−15.
   - Length of intervals between optical slices in a Z-stack: up to 8 μm.
   - Image size per tile (X,Y): 512 × 512 or 1024 × 1024 pixels/frame with a ~0.207 μm/pixel range when using a Zeiss LD C-Apochromat 40X/1.1 water Korr M27 objective.
   - Single 4-D stack acquisition time for complete migration: 5−10 min for 512 × 512 pixels and 10−15 min for 1024 × 1024 pixels images. These times can be considerably reduced (3−5 min) when using a lower magnification. Informative time lapses for scoring defects in migration speed or directionality can be recorded with a 10x objective, even though the cellular resolution will be low.
   - Image speed acquisition: 7−8 (2−4 microsec/pixel dwell) with averaging 1x. This parameter will vastly change based on the fluorescent marker used.

- Interval between each 4-D stack: 1–2 min. This is the designated time break between two Acquisition Cycles.
- Total time-lapse acquisition (*t*): 12–24 h.

2.5 POST TIME-LAPSE ANALYSIS

In the event that a specific experiment requires post time-lapse analysis, it is necessary to remove the imaged embryo from the agarose without causing any damage.

2.5.1 When embryos are kept alive

As embryos grow they must be released from the agarose after imaging to allow for proper development and tail elongation. Gently free the embryo from the agarose by carving it out of the agarose with a pair of forceps and transfer it into a dish containing fresh 0.5X E2 medium (without Tricaine). Pipette the embryo up and down with a fire-polished glass pipette until all the agarose surrounding the embryo loosens up and the embryo is completely free. Embryos can be remounted for renewed imaging if needed.

2.5.2 When embryos are fixed (for in situ hybridization, immunohistochemistry, etc.)

Time-lapsed embryos can be fixed for genetic analysis or nonvital labeling while still embedded in agarose by exchanging the 0.5X E2 medium with 3 mL of 4% paraformaldehyde (PFA) followed by an overnight incubation at 4°C. Once fixed, the embryos can be carefully dissected from the agarose with a pair of forceps. Transfer embryos to a clean dish containing PBST (PBS—0.1% Tween) and gently pipette them up and down with a glass pipette until all the agarose surrounding the embryos loosens up.

- *For genotyping*, transfer the fixed embryos into a 96-well PCR plate containing 100 μL DNA lysis buffer (10 mM Tris–HCl pH 8.0, 50 mM KCl, 0.3% Tween 20, 0.3% NP-40, 1 mM EDTA) and follow gene-specific genotyping protocols.
- *For in situ hybridization or immunohistochemistry* follow detailed published protocols (Lauter, Soll, & Hauptmann, 2014; Moens, 2008a, 2008b; Thisse & Thisse, 2008, 2014; Welten et al., 2006). Commonly used lateral line markers and the cell population they are expressed in are listed in Table 3.

3. LIVE LABELING OF LATERAL LINE CELLS

The external location of the lateral line allows imaging of the lateral line under DIC optics (Dambly-Chaudiere et al., 2003; Kimmel et al., 1995). As described previously, transgenic lines expressing fluorescently tagged proteins in the lateral line are very helpful. Yet, a particular line or mutants might not be in a transgenic background, or double or triple labeling is desired. Therefore, the availability of additional live labeling techniques is crucial (Table 4).

Table 3 Common Marker and Pathway Genes Used in Lateral Line Development

Pathway	Marker Gene	Expressing Tissue During Development	References
Wnt/β-catenin target genes	*lef1*	Primordium leading region and deposited interneuromast cells	Aman and Piotrowski (2008), Lecaudey et al. (2008), Lush and Piotrowski (2014a, 2014b), Matsuda et al. (2013), McGraw et al. (2011) Nechiporuk and Raible (2008), Pezeron et al. (2006), Valdivia et al. (2011), and Venero Galanternik et al. (2015)
	sef	Primordium leading region	
	axin2	Primordium leading region	
	fgf3	Primordium leading region and neuromasts (NM)	
	fgf10a	Primordium leading region and NMs	
	glypican1b	Small group of cells in tip of primordium	
	wnt10a	Primordium leading region	
	sfrp1a	All primordium cells, NMs, and interneuromast cells	
	rspo3	Primordium leading region	
	dusp6	Primordium leading region (also Fgf dependent)	
Fgf target genes	*dkk1b*	Boundary between leading and trailing primordium region	Aman and Piotrowski (2008), Ernst et al. (2012), Lecaudey et al. (2008), Lush and Piotrowski (2014a, 2014b), Nechiporuk and Raible (2008), and Venero Galanternik et al. (2015)
	pea3	Trailing primordium region	
	fgfr1	Trailing primordium region	
	atoh1a	Hair cell marker in primordium and NMs. Also Notch dependent	
	glypican4	Primordium trailing region, NMs, and interneuromast cells	
	syndecan3	Primordium trailing region	
	syndecan4	Primordium trailing region and NMs	
	shroom3	Region in the primordium where a protoneuromast forms	

Continued

Table 3 Common Marker and Pathway Genes Used in Lateral Line Development—cont'd

Pathway	Marker Gene	Expressing Tissue During Development	References
Chemokine	*cxcr4a*	Primordium leading region and NMs	Aman and Piotrowski (2008), David et al. (2002), Dona et al. (2013), Li, Shirabe, and Kuwada (2004), Valentin et al. (2007), and Venkiteswaran et al., 2013
	cxcr4b	Primordium leading region and NMs	
	cxcr7b	Primordium trailing region, NMs, and interneuromast cells	
	cxcl12a	Secreted by muscle precursors cells along the myoseptum	
Unknown	*eya1*	All lateral line cells	Aman and Piotrowski (2008), Grant et al. (2005), Nechiporuk and Raible (2008), and Venero Galanternik et al. (2015)
	s100t	Hair cells	
	klf17	Primordium and NM cells	
Notch Pathway	*deltaA*	Hair cell precursors in primordium and NMs	Itoh et al. (2003), Matsuda and Chitnis (2010), Romero-Carvajal et al. (2015), Wada et al. (2013) and Yeo, Kim, Kim, Huh, and Chitnis (2007)
	deltaB	Hair cell precursors in primordium and NMs	
	deltaC	hair cell precursors in primordium and NMs	
	deltaD	Hair cell precursors in primordium and NMs	
	notch1a	Support cells in primordium and NMs	
	notch1b	Support cells in primordium and NMs	
	notch3	Support cells in primordium and NMs	
	her4.1	Support cells in primordium and NMs	
	dkk2	Support cells in primordium and NMs—also an Fgf target	
ErbB	*erbb2*	Lateral line Schwann cells	Lush and Piotrowski (2014a, 2014b), Lyons et al. (2005), and Perlin, Lush, Stephens, Piotrowski, and Talbot (2011)
	erbb3b	Lateral line Schwann cells	
	neuregulin1-3	Lateral line axons	

Table 4 A Selection of Cell Type Specific Markers Used in Lateral Line Studies

Cell Type/Structure	Type of Marker	Marker	References
Hair cells and hair cell precursors	Gene expression	*atoh1a* *et4 (atp2b1a)* *s100t* *myoVIb* *deltaD* *deltaB* *deltaC*	Itoh and Chitnis (2001), Jiang et al. (2014), Matsuda and Chitnis (2010), Romero-Carvajal et al. (2015), and Venero Galanternik et al. (2015)
	Vital dyes	DASPEI (Thermo Fisher—D1306) FM 4–64/FM 4–64FX (Thermo Fisher—T-3166/F-34653) FM 1–43/FM 1–43FX (Thermo Fisher—T-3163/F-35355)	Kindt et al. (2012) and Nagiel et al. (2008)
Mantle cells	Transgenic line	*Tg(krt4:EGFP)^{sET20}* *Tg(−4.7alpl:mCherry)^{ru1011}*	Parinov et al. (2004) and Steiner et al. (2014)
Mantle and support cells surrounding the hair cells	Endogenous enzymatic activity	Alkaline phosphatase	Lush and Piotrowski (2014a, 2014b) and Villablanca et al. (2006)
	Gene expression	*tcf4* *cxcr7b* *sfrp1a*	Jiang et al. (2014), Pezeron et al. (2006) and Valentin et al. (2007)
Apical constrictions	Antibodies	γ-Tubulin (Sigma–Aldrich—T-3559) F-actin/Phalloidin 488/568 (Thermo Fisher—A12379/A12380) ZO-1 (Thermo Fisher) αPKCζ (Santa Cruz Biotechnologies—sc-216)	Ernst et al. (2012), Hava et al. (2009), and Lecaudey et al. (2008)

Continued

Table 4 A Selection of Cell Type Specific Markers Used in Lateral Line Studies—cont'd

Cell Type/Structure	Type of Marker	Marker	References
		Phospho-myosin light chain 2 (Cell Signaling—3671P)	
		Rock2a (Anaspec—55431s)	
		Myo-II	
	Transgenic line	*TgBAC(cdh2:cdh2-GFP)*	Haas and Gilmour (2006) and Revenu et al. (2014)
		Tg(claudinB:lynGFP)^{zf106}	
	Gene expression	*par3*	Ernst et al. (2012) and Hava et al. (2009)
		lgl2	
		prkci	
Nascent protoneuromast in primordium	Gene expression	*shroom3*	Ernst et al. (2012)
All embryo cells	Nuclear and apoptotic markers	DAPI (Thermo Fisher)	Hava et al. (2009), Santos, MacDonald, Rubel, and Raible (2006), and Venero Galanternik et al. (2015)
		TO-PRO/YO-PRO (Thermo Fisher)	
		BODIPY (Thermo Fisher)	
Muscle markers (muscle influences primordium migration)	Antibodies	4D9—Engrailed (Santa Cruz Biotechnologies—sc-53019)	Dolez, Nicolas, and Hirsinger (2011) and Venero Galanternik et al. (2015)
		Anti-focal adhesion kinase (pFAK^{Y397}) (Thermo Fisher—44-626G)	Subramanian and Schilling (2014)
		Anti-Laminin (Sigma–Aldrich—L-9393)	Dolez et al. (2011), Subramanian and Schilling (2014)
	Gene expression	*cxcl12a*	David et al. (2002)
		dystrophin	Jurynec et al. (2008)
	DIC/Nomarski Optics	Visualization of unstained structures using enhanced interference contrast	Kimmel et al. (1995)

3.1 LABELING LATERAL LINE WITH VITAL DYES

The following methods describe reagents that label cell structures of the lateral line in live embryos.

3.1.1 BODIPY 505/515 and BODIPY-ceramide staining

These lipid-based vital fluorophores are a convenient alternative to label all cell membranes, for example, in mutants that have not yet been crossed with transgenic lines. These dyes allow for confocal live imaging for up to 10 h without suffering serious photobleaching (Cooper, D'Amico, & Henry, 1999; Cooper et al., 2005). However, for better lateral line staining, embryos should be incubated in BODIPY overnight.

3.1.2 DASPEI and FM lipophilic dyes

The fluorescent mitochondrial labeling dye DASPEI (2-(4-dimethylaminostyryl)-N-ethylpyridinium iodide) and the lipophilic fixable membrane-labeling dyes FM 1−43 and FM 4−64 are extensively used vital dyes in zebrafish and other aquatic species to label lateral line sensory hair cells, ganglia, and neurons and are employed to assess hair cell function (Grant et al., 2005; Harris et al., 2003; Kindt, Finch, & Nicolson, 2012; Lush & Piotrowski, 2014a; Nagiel, Andor-Ardo, & Hudspeth, 2008).

DASPEI staining is a quick and powerful tool for the characterization and identification of new zebrafish mutants affecting hair cell development or regeneration. To label sensory hair cells by DASPEI or FM dyes in the embryo prepare:

- Live 3−5 dpf embryos. In younger embryos (48 hpf) the staining might be weak because only differentiated hair cells are labeled.
- 0.5X E2 medium—2 mL/sample.
- 0.06 mg/mL DASPEI (Thermo-Fisher—D-426) solution in 0.5X E2 medium—2 mL/sample or
- 3 μM FM 1−43 (Invitrogen) solution in 0.5X E2 medium—2 mL/sample or
- 100 μM FM 4−64 (Invitrogen) solution in 0.5X E2 medium.
- 0.5X E2 medium plus 130 μL Tricaine (MS-222—4 g/L pH 9.0)—2 mL/sample.
- Embryo transfer baskets.
- 24-well plate.

1. Assign three wells per sample in a 24-well dish.
2. Place embryos (10−15) into a transfer basket and submerge them in the first well containing 0.5X E2 medium.
3. *For DASPEI*: Transfer the basket into the second well containing the DASPEI solution and incubate for 10 min at room temperature.
   For FM 1−43: Transfer the basket into the second well containing the FM 1−43FX solution and incubate for 20 s at room temperature in the dark.
   For FM 4−64: Transfer the basket into the second well containing the FM 4−64FX solution and incubate for 2 min at room temperature in the dark.

4. Remove the basket from the staining solution and briefly rinse the embryos with 0.5X E2 medium.
5. Place the basket in the third well containing 0.5X E2 plus Tricaine and incubate for 2–3 min. Do not expose embryos to Tricaine before soaking them in DASPEI, as Tricaine inhibits its uptake.
6. *Image DASPEI* positive hair cells under a GFP (488 nm) or a long-pass GFP (~500 nm) filter. We prefer the long-pass filter, as hair cells appear brighter and can be imaged in conjunction with other GFP-labeled proteins.
   Image FM stained hair cells under an RFP/mCherry filter (568 nm).
7. *DASPEI* will be metabolized by the embryo, therefore image acquisition or phenotype scoring needs to be performed promptly after staining (within a 30 min window).
   Fixable (FX) *FM 1–43 and FM 4–64* versions can be detected with most immunostaining protocols allowing the staining and imaging of more embryos.
8. Individual, low magnification images can be stitched using ImageJ.

3.2 CELL LINEAGE TRACING AND CLONAL ANALYSIS BEHAVIOR

We discuss several methods to label individual or small clusters of cells within the lateral line and their applications.

3.2.1 Transplantations

Transplantations of labeled donor cells into an unlabeled blastula-stage host embryo are a powerful method for labeling and investigating the behavior of single or small groups of cells (Li, White, & Zon, 2011). Transplantation of small groups of cells allows the study of their behavior, which would not be possible if all cells were labeled. A second purpose of transplantations is to determine if a gene functions cell-autonomously or noncell-autonomously. For example, primordium migration does not only depend on signals active within the primordium, like Wnt/β-catenin and Fgf signaling and chemokine receptor expression, but it is also affected by loss of guidance molecules, such as *cxcl12a* in muscle cells along the myoseptum (Aman & Piotrowski, 2008; David et al., 2002; Haas & Gilmour, 2006; Lecaudey et al., 2008; Nechiporuk & Raible, 2008). Hence, in mutants in which the primordium stalls, it is essential to show whether the mutated gene acts in the primordium or in the environment.

A rough fate map for lateral line placodes has been described and donor cells should be injected into this area of the host in order to obtain lateral line clones (Kozlowski, Murakami, Ho, & Weinberg, 1997). As the anterior–posterior axis of the embryo cannot be distinguished until the shield stage (6 hpf), placing donor cells in two positions in the host embryo often increases the chances of obtaining clones in the posterior lateral line placode. Alternatively, to facilitate the identification of the dorsal side before gastrulation, the use of a transgenic line in which GFP is expressed under the *goosecoid* promoter enables the correct localization of the dorsal shield (Carmany-Rampey & Moens, 2006).

For details, please refer to published transplantation protocols (Carmany-Rampey & Moens, 2006; Kemp, Carmany-Rampey, & Moens, 2009; Li et al., 2011).

3.2.2 mRNA and DNA microinjections

Embryos can be microinjected with mRNAs encoding for proteins that label different cellular compartments, such as membranes, nuclei, or the cytoplasm in all cells of the embryo. mRNA injections are useful for the analysis of nontransgenic embryos, to label cellular compartments not labeled in transgenic lines, or when double labeling is required for colocalization assays.

In contrast to mRNA microinjections that result in the global expression of a protein in the embryo, injection of DNA leads to mosaic expression and labels many fewer cells. However, the chances that cells are labeled in your tissue of interest are much lower, especially if the tissue consists of relatively few cells, such as the lateral line. Therefore, transplantation of mRNA-containing donor cells is often more efficient to obtain lateral line clones. For detailed application of this methodology refer to previously published work (Hogan, Verkade, Lieschke, & Heath, 2008).

3.2.3 Photoconvertible fluorescent proteins

Photoconversion of small groups or single cells within the primordium is aimed at determining cell fates and cell rearrangements that occur during migration (Breau, Wilkinson, & Xu, 2013; McGraw, Culbertson, & Nechiporuk, 2014; McGraw et al., 2011).

Since the discovery of the photoconvertible protein Kaede in the stony coral *Trachyphyllia geoffroyi* (Ando, Hama, Yamamoto-Hino, Mizuno, & Miyawaki, 2002), many other proteins such as Dendra, KikGR, and Dronpa that switch from green to red fluorescence upon exposure to violet or UV light have been characterized (Ando, Mizuno, & Miyawaki, 2004; Gurskaya et al., 2006; Tsutsui, Karasawa, Shimizu, Nukina, & Miyawaki, 2005). These photoconvertible proteins have been employed in zebrafish cell lineage studies and detailed protocols are available (Hatta, Tsujii, & Omura, 2006; Lombardo, Sporbert, & Abdelilah-Seyfried, 2012; Schuster & Ghysen, 2013). Expression of photoconvertible proteins in the lateral line can be achieved by microinjection of mRNA of nuclear or cytoplasmic localized *Kaede* or by the use of stable Kaede transgenic lines (see Table 1). To facilitate the identification of lateral line cell populations, photoconversion experiments can be performed in the *Tg(cldnb:lynGFP)* line.

The following protocol utilizes nuclear localized Kaede *(nlsKaede)* microinjection and a confocal microscope to UV-irradiate the primordium. However, photoconversion of small numbers of cells can also be achieved using the UV/DAPI filter on a compound microscope and mounting embryos in 2% methylcellulose (in 0.5X E2 medium) on a glass slide covered by a coverslip. If a compound microscope is used, the photoconverted region will correspond to the field of view, hence, the higher the magnification, the smaller the area that will be UV-exposed.

Note: Preferably perform the tasks described in this protocol in a dark room and avoid any exposure to UV light, including natural light.

1. Microinject 1−2 cell stage embryos with 1−2 nL of a *nlsKaede* mRNA (1 μL of mRNA, 1 μL 0.5% Phenol red solution—Sigma−Aldrich, 3 μL RNAse free water).
2. Culture embryos in the dark at 28.5°C until the appropriate stage.
3. Select green, Kaede-expressing embryos and dechorionate them.
4. Anesthetize and mount the embryos in LMP agarose (following the protocol described previously).
5. Locate the lateral line. We use a Zeiss LD C-Apochromat 40X/1.1 water Korr M27 objective.
6. Select the area to be irradiated/bleached. This area can be as small as a single cell or the entire primordium. Converting single cells is more challenging and often 2−3 cells are photoconverted.
7. Expose the selected region to a single initial pulse of 5% of 30 mW 405 nm laser with 150−180 times of iteration.
8. Detect the photoconverted red and original green Kaede protein by using the 561 and 488 nm lasers, respectively. In the event that the photoconversion was incomplete or unsatisfactory, repeat the bleaching pulse on Step 8.
9. Set up time lapse.

4. NONVITAL TISSUE LABELING OF LATERAL LINE CELLS

In fixed, nontransgenic manipulated or mutant embryos the lateral line can be labeled by in situ hybridization and immunohistochemistry techniques (Tables 2 and 3) (Lauter et al., 2014; Moens, 2008a, 2008b; Thisse & Thisse, 2008, 2014). These techniques are robust, however, they take a couple of days to be completed. The following nonvital staining methods allow a quick and informative assessment of lateral line migration in uncharacterized nontransgenic mutants or manipulated embryos.

4.1 NUCLEAR LABELING WITH 4′,6-DIAMIDINO-2-PHENYLINDOLE

4′,6-Diamidino-2-phenylindole (DAPI) labels all cell nuclei fluorescently and is a fast way to characterize lateral line development in whole embryos under a UV filter. It is not specific for the lateral line, but cell nuclei are close to each other in the lateral line, distinguishing them from surrounding tissues. DAPI binds to A-T rich regions of DNA and is more effective in fixed tissues (Chazotte, 2011). Because the main goal of this staining is to reveal potential problems with lateral line development, it is recommended to perform this staining at around 48 hpf, when the primordium has completed migration and has deposited five to six neuromasts along the trunk. Perform all following steps at room temperature:

- Fix dechorionated embryos with 4% PFA for 2−4 h.

- Wash 3 times with PBST (1X PBS, 0.1% Tween) for 10 min.
- Incubate in a DAPI solution (1:1000 in PBST) for 1 h for 48 hpf and 2 h for 5 dpf embryos.
- Wash 3 times with PBST for 5 min.
- Mount individual embryos in a drop of 2% or 6% methylcellulose (in 0.5X E2) for 48 hpf or 5 dpf, respectively, on a glass slide covered by a coverslip (# 1.5).
- Image the labeled lateral line on a compound or confocal microscope under a UV/DAPI filter using 5–63X objectives.

4.2 ALKALINE PHOSPHATASE STAINING

This whole-mount staining allows for the fast visualization of the deposited neuromasts and assessment of their location across the embryo trunk (Fig. 1K). Also, neuromast hair cells remain unstained in the center of the neuromast providing clues on whether an embryo possesses sensory hair cells or not.

1. Fix 3–5 dpf embryos in 4% PFA overnight at room temperature.
2. Wash the embryos 3×5 min each in PBS/0.3% Tween-20 followed by 3×5 min washes in staining buffer (50 mM $MgCl_2$, 100 mM NaCl, 100 mM Tris pH 9.5%, and 0.1% Tween-20).
3. Place embryos in staining buffer plus 3.4 μL/mL NBT and 3.5 μL/mL BCIP (Roche, USA) and stain at room temperature in the dark, evaluating the staining process every 10 min.
4. Stop the staining reaction by rinsing the embryos with PBS/0.3% Tween-20 and fixing them with 4% PFA.

4.3 PHALLOIDIN STAINING

F-actin accumulates in the apical constrictions of neuromast cells and also labels the actin-rich stereocilia of the sensory hair cells. However, it does not label the microtubule-based kinocilia, which are localized to one pole of the hair cells (Fig. 1I–J and L–M′). Thus, Phalloidin staining allows the assessment of hair cell polarity by measuring the orientation angles of each hair cell in a neuromast (see the later discussion).

1. Fix embryos in 4% PFA overnight at 4°C or at room temperature for 2 h. Do not use methanol-treated embryos as methanol destabilizes actin.
2. Wash 2x for 5 min in PBSTx (1X PBS + 0.2% Triton X-100).
3. Permeabilize the embryos by washing them 4x for 30 min in PBS + 2% Triton X-100.
4. Wash 2x for 5 min in PBSTx (1X PBS + 0.2% Triton X-100).
5. Prepare a 1:40 Phalloidin solution (Invitrogen, Alexa 488- or Alexa 568-conjugated) in PBSTx.
6. Incubate in 200 μL for 2 h at room temperature in the dark.
7. Rinse briefly in PBSTx.

8. Wash 3x for 40 min in PBSTx and proceed to image within 1−2 days.
9. To assess apical constrictions in primordium rosettes and deposited neuromasts, image the entire tail of the embryo under a compound or confocal microscope at a 10−20X magnification. For hair cell polarity assessment, image on a confocal microscope using a 40/63X objective.

5. INTERPRETATION OF COMMON PHENOTYPES

Mutant analyses provided us with a basic understanding of the signaling pathways that coordinate primordium migration, neuromast formation and deposition (Chitnis et al., 2012; Thomas et al., 2015). Therefore, the observation of particular phenotypes should be followed up by gene expression analyses of the pathways that were previously described to cause similar defects (Tables 2 and 4). Some of the most common phenotypes are:

1. **Stalling of the primordium**: Failure of the primordium to reach the tail tip is often associated with defects in chemokine signaling. Proper chemokine signaling depends on the normal expression of the chemokine ligand *cxcl12a* in muscle cells along the myoseptum, as well as on the normal distribution of the chemokine receptors *cxcr4b/cxcr7a* within the primordium. The distribution of chemokine receptors in the primordium is in turn regulated by interactions between the Wnt/Fgf pathways. Therefore, one has to determine if the migration defect could be secondary to defects in trunk muscle development or if chemokine signaling within the primordium is affected (Aman & Piotrowski, 2008; Dalle Nogare et al., 2014; Haas & Gilmour, 2006; Meyers et al., 2013; Nechiporuk & Raible, 2008).
2. **Deposition of fewer and further spaced neuromasts**: Deposition defects are the most often described phenotypes. Unfortunately, deposition defects are a common result of cell death in the primordium (Aman et al., 2011). Cell death in the primordium is a side effect of injections of toxic morpholinos, however, can also be caused by mutations in genes that cause cell death in the nervous system. How neuromast deposition is regulated is not well understood. However, neuromast deposition is affected by proliferation and primordium migration speed and these parameters should be quantified when a deposition defect is reported (Aman et al., 2011; Matsuda et al., 2013).
3. **Failure of protoneuromast formation in the primordium**: The formation of rosette-shaped protoneuromasts within the primordium depends on Fgf-induced cell shape changes (Ernst et al., 2012; Harding, McGraw, & Nechiporuk, 2014; Harding & Nechiporuk, 2012; Lecaudey et al., 2008). In addition, *lgl2* and *prkci* are involved in the maturation of apical constrictions (Hava et al., 2009). Table 3 lists markers and genes for apical constrictions.
4. **Extra neuromast formation**: Precocious development of postembryonic neuromasts is caused by the loss of an inhibitory signal from Schwann cells to

lateral line cells (revised by Goodrich, 2005; Whitfield, 2005). Therefore, the phenotype is induced by manipulations or mutations that lead to the loss of Schwann cells or loss of the lateral line axons along which Schwann cells migrate. Alternatively, the inhibitory signal or its receptor that have not yet been identified could be affected (Lush & Piotrowski, 2014a).

6. HAIR CELL REGENERATION

Like lateral line hair cells, inner ear hair cells are susceptible to environmental insult. For example, inner ear hair cells are sensitive to loud noise, infections, antibiotic drugs, and chemotherapeutic agents, which cause hair cell death resulting in sensory-neural deafness and balance disorders (Furness, 2015). In contrast, non-mammalian vertebrates, like fish, amphibians, reptiles, and birds, replace hair cells throughout life. Zebrafish lateral line cells regenerate their hair cells within 72 h after hair cell death (Ma, Rubel, & Raible, 2008; Romero-Carvajal et al., 2015). In zebrafish and chicken, hair cells are replaced from dividing support cells (Fig. 1N) (Harris et al., 2003; Hernandez, Olivari, Sarrazin, Sandoval, & Allende, 2007; Ma et al., 2008; Mackenzie & Raible, 2012; Wibowo, Pinto-Teixeira, Satou, Higashijima, & Lopez-Schier, 2011). However, even in these regenerating species the cellular and molecular mechanisms underlying this regenerative ability are yet to be fully understood (Brignull, Raible, & Stone, 2009). Zebrafish neuromasts possess several support cell populations (Cruz et al., 2015; Ma et al., 2008; Romero-Carvajal et al., 2015; Wibowo et al., 2011). Long-term in vivo tracking of all dividing support cells during regeneration, coupled with cell fate analyses revealed the existence of self-renewing progenitor cells in the poles and differentiating support cells in the center of the sensory organs (Romero-Carvajal et al., 2015). A basic network between Notch and Wnt signaling is fundamentally important for maintaining the balance of these two support cell types ensuring the life-long ability to regenerate hair cells. Here we are describing powerful assays that allow the functional interrogation of as yet undescribed gene interactions that regulate the balance of progenitor cell self-renewal and differentiation at the single cell level.

7. LONG-TERM TIME-LAPSE ANALYSES OF REGENERATING NEUROMASTS

Imaging 5 dpf neuromasts for up to 72 h poses several challenges:

- Larval survival and immobilization are more difficult to achieve at 5 dpf.
- Because neuromasts have to be imaged at high magnification to obtain cellular resolution, the chances of specimen drift are high during long time-lapse recordings.

- Finally, constant imaging of homeostatic and regenerating neuromasts leads to bleaching of the fluorescence of transgenes over time.

The following protocol has been optimized for larval survival, immobilization, and sampling of mitotic events during neuromast homeostasis and regeneration for up to 72 h. Imaging of regenerating neuromasts requires that they are immobilized/anaesthetized first before killing the hair cells.

7.1 IMMOBILIZATION

As described for embryos, immobilization of five dpf larvae is achieved by immersing them in the anesthetic Tricaine methanesulfonate (MS-222). However, larvae become much more sensitive to Tricaine between 4 and 7 dpf due to a switch in the site of ion regulation and detoxification from the skin to the gills (Rombough, 2007). Therefore, Tricaine becomes extremely lethal at higher doses after 4 dpf and caution must be used when treating the larvae.

Follow these steps carefully to assure survival:

1. To reduce lethality during recording, start by adding 100 μL of Tricaine (4 g/L, pH 7.4) to a 100 mm × 50 mm Petri dish containing the larvae in 50 mL of 0.5X E2 media and stir the dish to mix.
2. Test if larvae are immobilized by their response to mechanical stimulation before adding more Tricaine. Add 100 μL of Tricaine every 20 min until larvae become unresponsive to touch or up to 100 mg/L. Commonly, complete immobilization is reached after 3 h. Importantly, the effective dose of Tricaine varies between experiments.
3. Mount one or two 5 dpf larvae on their sides in a MatTek dish using 1% LMP in 0.5X E2 medium agarose containing Tricaine, as described for embryos previously.

   Notes: We highly recommend adding the Tricaine in increments, as adding the total concentration of Tricaine at once will kill the larvae. Once the larva becomes unresponsive, mount the larva or treat it with neomycin to induce hair cell death (see the later discussion).

7.2 HAIR CELL DEATH

To kill neuromast hair cells and trigger a regenerative response several reagents, such as aminoglycoside antibiotics, cisplatin, or copper can be used (Mackenzie & Raible, 2012; Ou, Raible, & Rubel, 2007). We prefer killing hair cells with the antibiotic Neomycin Sulfate (Fisher Bioreagents) as it acts within minutes without killing any support cells or damaging the neuromast structure (Mackenzie & Raible, 2012). Before killing hair cells, the larvae should already be completely immobilized, which can take up to 3 h, as described previously.

Note: Keep 300 mM Neomycin Sulfate stocks in small aliquots (10−20 μL) frozen at −80°C. Do not refreeze the stocks.

1. Use embryo baskets to transfer up to 20 larvae to a 2 mL well (6-well plates) containing 300 μM neomycin in 0.5X E2 plus Tricaine.
2. Incubate in neomycin solution for 30 min at 28.5°C in the dark.
3. Rinse three times in 0.5X E2 medium plus Tricaine.
4. Neomycin-treated embryos should be mounted immediately after 0.5X E2 rinses.

7.3 TIME-LAPSE ANALYSIS AND TRACKING OF SUPPORT CELLS DURING REGENERATION

During regeneration of wild-type primI-derived neuromasts, support cells self-renew in the dorsoventral poles and differentiate into hair cells in the center. In primII-derived neuromasts support cells self-renew in the antero-posterior poles. To test the effect of particular genes on hair cell regeneration, time-lapse recordings are useful. For example, if manipulation of a gene causes a reduction in hair cell regeneration, time-lapse recordings will reveal whether hair cell precursors are specified but fail to differentiate, or whether these hair cell precursors die. Live imaging will also reveal if hair cell precursors fail to rearrange themselves after division, a process that is important for establishing hair cell polarities (Mirkovic, Pylawka, & Hudspeth, 2012; Wibowo et al., 2011).

To image mitotic events, hair, support, and mantle cells should be labeled with a combination of transgenes. This can be achieved by crossing the double transgenic lines *Tg(cldnb:lynGFP); Tg(cldnb:H2A-mCherry)* and *Et(krt4:EGFP)^{sqet20}; Et(krt4:EGFP)^{sqet4}* (Table 1, Fig. 1A–H). A protocol for time-lapse imaging of neuromasts using a light sheet microscope is available (Pinto-Teixeira et al., 2013), however, we prefer imaging under a conventional confocal microscope as we have no problems with photobleaching and the data analysis is less complex.

7.3.1 Spatial sampling (setting up the Z-stack)

When a 5 dpf larva is mounted on its side, the primI-derived neuromasts of the posterior lateral line are well-positioned for live imaging as they will be lying flat and close to the glass bottom. This is important to avoid drifting and improving image quality for long-term time-lapse imaging. Neuromasts are circular organs and their diameter ranges between 30 and 40 μm. Cells within neuromasts are densely packed and the nuclei of support cells are located more basally in the sensory organ than the hair cell nuclei, giving the appearance of a pseudostratified epithelium. The approximate height of a mature neuromast is 10–13 μm. During mitoses of amplifying support cells and mantle cells, the nuclei move apically and the daughter cells move back basally, resembling interkinetic nuclear migration. The nuclei of newly formed hair cells, on the other hand, remain in the upper nuclear layer and undergo a rotating rearrangement during differentiation (Lopez-Schier et al., 2004; Mirkovic et al., 2012). Accordingly, the Z-stack should encompass the whole neuromast height plus extra space above and below (approximately from the tips of the protruding cilia to the muscle underlying the neuromasts).

7.3.2 Recording time and time sampling

The analysis of homeostatic and regenerating neuromasts revealed that the vast majority of proliferating cells in a neuromast are the support cells. Mantle cells divide rarely and hair cells are not proliferative (Romero-Carvajal et al., 2015). Mitoses in 5 dpf homeostatic neuromasts are scarce with approximately one amplifying cell division and one differentiating cell division every 24 h. During regeneration the proliferation rate doubles and is maintained until the original number of hair cells is restored, approximately 48 h after hair cell death. During regeneration, some support cells divide twice. In these cases, one of the daughter cells differentiates while the other remains quiescent. To sample rare events such as mantle cell divisions or a second support cell division, neuromast regeneration should be recorded for more than 48 h. This time frame also allows determining which daughter cell remains as a support cell and which one differentiates into hair cells.

Mitosis lasts about 30 min from the moment the nucleus moves apically until cytokinesis; however, the transition from metaphase to cytokinesis only lasts about 10 min. As dividing support cells look like any other support cell before metaphase and after telophase, in our hands time sampling of about 6 min ensures that no cell divisions are missed.

7.3.3 Suggested parameters for time-lapse recordings of regenerating neuromasts

- Imaging can be performed on a conventional laser scanning confocal microscope, preferably with a 40X long-working distance water objective (such as a Zeiss LD C Apochromat 40x/1.1 water Korr M27) and a 2.5X optical zoom.
- An imaging frame of 512 × 512 pixels is sufficient to record a single neuromast and account for its possible drift along the X,Y planes.
- The dimensions of the Z-stack should be approximately 20−23 μm with a depth of 0.9 μm per section.
- Laser intensity must be kept low and the scanning speed must be increased compared to still image acquisitions to avoid bleaching of the fluorescence and to keep time-sampling intervals under 10 min.

7.4 IMAGE PROCESSING AND LINEAGE TRACKING

While time lapses of confocal Z-stacks can be analyzed in any software, for example, ImageJ, lineage analyses and movie rendering is easier in Imaris (Bitplane). Imaris provides a user-friendly way to extract positional data for quantitative cell movement and spatial analysis of proliferating cells (Fig. 4, see the later discussion).

1. To track nuclei positions and lineages, use the Imaris spot function, which provides positional information of the tracked cell within the Z-stack (X_n, Y_n; Fig. 4A).

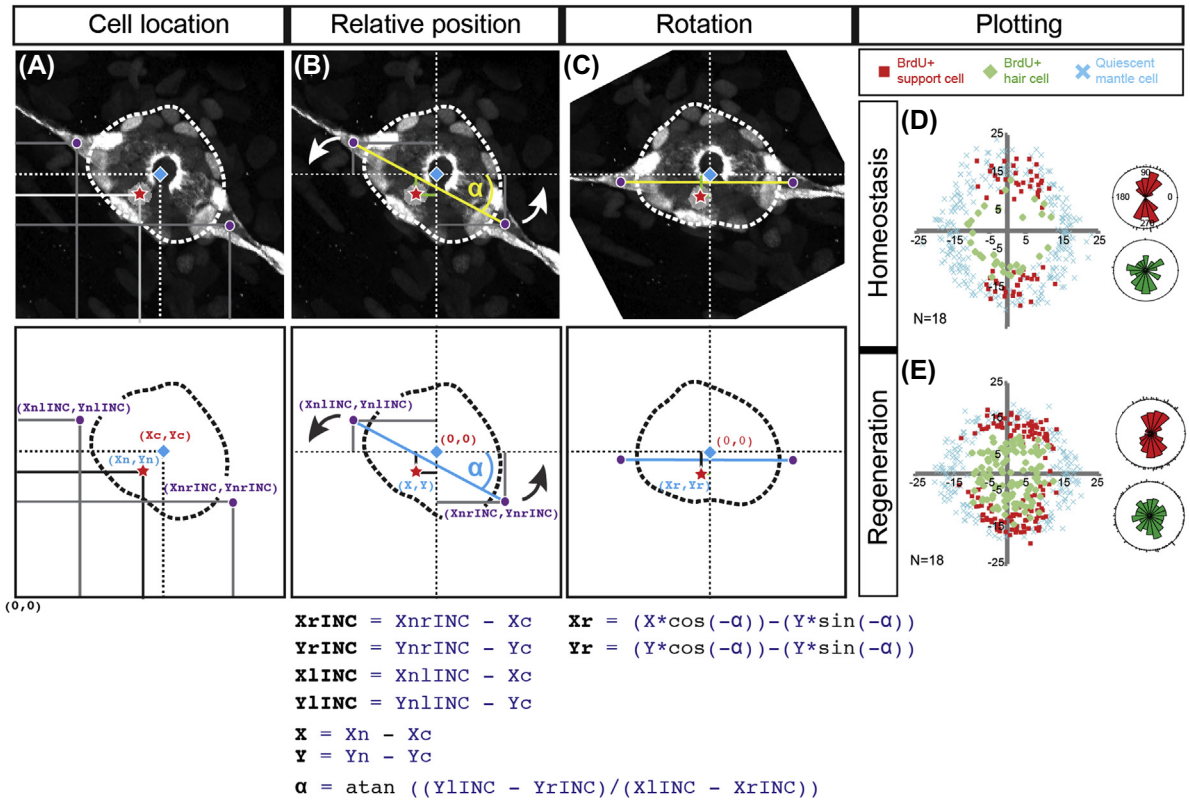


FIGURE 4 Spatial analysis of dividing BrdU-positive amplifying and differentiating support cells.

(A) First, the position of the center of the neuromast (*blue diamond* (light gray in print versions)) and the left and right interneuromast cells (INCs, *purple circles* (dark gray in print versions)) are determined. The *red star* (gray in print versions) represents the position of the cell of interest. (B) Next, the coordinates (0,0) are assigned to the center, and every other coordinate is determined relative to this point. To standardize the horizontal plane, the relative positions of the INCs provide the tilt angle (**α**) for rotation of the data. (C) Once the neuromast is centered (0,0) and adjusted to a universal horizontal plane, all the cells of interest are plotted and overlaid to visualize their localization. (D–E) Dot plots show the positions of mantle cells (*blue crosses* (gray in print versions)), BrdU+ amplifying (*red squares* (dark gray in print versions)), and differentiating support cells (*green squares* (light gray in print versions)) during homeostasis and regeneration. The rose diagrams show the polarized distribution of the amplifying support cells within the dorsoventral poles of the neuromast. In contrast, dividing support cells that differentiate into hair cells are not biased toward any of the poles.

2. To determine the fate of the dividing cell, the daughter cells are tracked until the end of the time-lapse movie by following their nuclei in the Z-stacks across time.
3. To determine the original position of a hair cell or support cell progenitor, the dividing support cells can be manually backtracked to the beginning of the movie.

7.5 CELL MOVEMENT ANALYSIS

In wild-type neuromasts, support cells do not move much along the X- and Y-axes. However, to determine if cells behave differently in mutant or manipulated neuromasts, the cell displacement of every mitotic cell and its progeny within a neuromast can be measured. Analyzing the first 25 h after hair cell death is sufficient, as most divisions occur during that time.

7.5.1 Parameters

(X_n, Y_n) = The position of the n^{th} neuromast cell
(X_c, Y_c) = The position of the center
t_m = Time at mitosis
$(Xt_m + 25,\ Yt_m + 25)$ = Position at 25 frames after mitosis

1. Create a center-stabilized movie overlaid with color-coded cell divisions:
   a. Tracking the geometrical center (X_c, Y_c) of a neuromast creates a stabilized reference point for the overlay of multiple neuromasts and creates drift-free time-lapse recordings. Track the geometrical center of the neuromast across time by manually drawing the contour of the neuromast using the Imaris surface tool. Once all surfaces are created, Imaris will calculate the geometrical center (X_c, Y_c) of the neuromast surface for each time point. Export the position data to a spreadsheet from the "statistics" tab.
   b. To calculate the relative position of the mitotic cell of interest to the center at each time point, subtract the geometrical center of the neuromast from the position of the mitotic cell in the image using the formula $X = (X_n - X_c)$, $Y = (Y_n - Y_c)$, where X_c, Y_c is the geometric center of the neuromast, and X_n, Y_n is the position of the n^{th} neuromast cell.
   c. To visualize the results, export the positional data for each cell over time to a spreadsheet and then overlay the positions on a stabilized version of the time lapse. To do this, we created a java program in ImageJ to plot the positional data on a 2D plane, effectively creating a Z-projection. The program creates an image for each time point by plotting the (X, Y) position of every cell as a colored spot. A separate image stack is created for each parental cell and its progeny. After the java program creates each image stack, all the stacks are imported into ImageJ. We also imported a Z-projected stack of the original fluorescence channels, center-stabilized to overlay the tracked cells onto the original image. Then we combine all of the image stacks into one, treating each stack as an individual channel. This allows coloring each channel differently so that daughter cells are labeled the same color as their parent

cells. The final result is an image stack containing the original fluorescence signal, with each added channel containing a colored dot on top of the tracked cells, and where each different color represents a specific progenitor cell and all its progeny.

2. Create a vector map containing vectors from the initial position of each progenitor cell to the final position of its progeny:
   a. To visualize the displacement over time, create a vector map using three data points from the same data obtained in Steps (1a) and (1b). Determine the relative position at time 0 (1 h post neomycin treatment) of each progenitor cell nucleus (Xt_0, Yt_0), the time of mitosis t_m, and the final position of one daughter cell after 25 time frames, which is approximately 3 h after mitosis $(Xt_m + 25,\ Yt_m + 25)$. As the two daughter cells usually stay in close proximity, tracking one of the daughter cells is sufficient.
   b. Based on these data, calculate the vector distance between the initial and final points, representing the total displacement of the mother−daughter cells. To illustrate displacement, plot the direction vectors using MS Excel, R, or other software that allows Cartesian plane plotting. Because the stabilized center calculated in part 1 was used, it is possible to overlay vector plots from different movies.

7.6 SPATIAL ANALYSIS OF THE ORIGIN OF SUPPORT AND HAIR CELL PROGENITORS IN FIXED LARVAE

To test the effect of particular genes on hair cell regeneration, time-lapse recordings are useful, however, their generation and analyses are time-consuming and only allow the study of relatively few neuromasts. Since cell displacement in the X, Y planes is negligible in regenerating neuromasts (Romero-Carvajal et al., 2015), BrdU incorporation for 24 h coupled with cell fate markers can be used to:

1. Reveal the spatial distribution of amplifying and differentiating support cell divisions.
2. Determine if cell fates are affected, resulting in too few or too many hair cells.

This approach is consistent with results obtained in time-lapse analyses (Romero-Carvajal et al., 2015). Because of the relative ease with which many neuromasts can be analyzed, this technique is suitable to test different mutants or larvae in which pathways have been manipulated. This protocol also allows to test the role of signaling pathways in determining cell behavior by treating larva with pharmacological inhibitors like the GSK3-β inhibitor and Wnt activator 1-Azakenpaullone (Sigma−Aldrich) and the γ-secretase inhibitor LY411575 (Selleckchem—S2714) that blocks Notch signaling (Romero-Carvajal et al., 2015).

Notes: Dilute pharmacological reagents in 100% DMSO and keep small stocks in small aliquots (10−20 μL) frozen at −80°C. Do not refreeze the stocks. Keep BrdU powder at −20°C and always prepare a fresh solution.

7.7 BrdU INCORPORATION

1. Pretreat larvae in 1% DMSO in 0.5X E2 for 6 h with or without drugs. The pretreatment ensures efficacy of the pharmaceutical treatments before inducing hair cell death and starting the BrdU incorporation.
2. Kill hair cells with neomycin. Use embryo baskets to transfer up to 20 larvae into a 2 ml well (6-well plates) containing 300 μM neomycin in 0.5X E2.
3. Incubate for 30 min at 28.5°C in the dark.
4. Rinse three times in 0.5X E2 medium.
5. Incubate for 24 h in 1% DMSO in 0.5X E2 plus 10 mM BrdU (Sigma–Aldrich—B5002) with or without pharmacological reagents.
6. Fix larvae in 4% PFA at 4°C until needed for immunohistochemistry (3 days to a week).

7.8 IMMUNOHISTOCHEMISTRY

This BrdU immunodetection protocol is a modification of Ma et al. (2008). All the steps should be carried out at room temperature except when noted otherwise.

For this protocol you will need:

- 1X PBST (PBS, 1% DMSO and 0.1% Tween)
- Methanol (30%, 60%, 100%) in 1X PBST
- Proteinase-K
- 4% PFA
- Distilled H_2O
- 2N HCL
- NGS (Normal Goat Serum)
- Anti-BrdU (Accurate Chemical & Scientific Corp)
- Rat Alexa Fluor 647 (Invitrogen/Fisher)
- Rabbit Alexa Fluor 488 (Invitrogen/Fisher)
- DAPI

1. Dehydrate fixed larvae in a methanol series of 30%, 60% up to 100% for 5 min each and store at −20°C overnight (O/N).
2. Rehydrate stepwise to 100% PBST.
3. Wash 3x in PBST, 5 min each.
4. Permeabilize larvae for 15 min with 20 μg/mL Proteinase-K in PBST without shaking.
5. Wash 3x in PBST, 5 min each.
6. Refix in 4% PFA for 30 min.
7. Wash 3x in PBST, 5 min each.
8. Wash 2x in distilled H_2O, 10 min each.
9. Treat larvae for 1 h in 2 N HCL in distilled H_2O without shaking.
10. Wash 3x in PBST, 5 min each.
11. Block for 1 h in PBST + 10% NGS.

12. Incubate for O/N at 4°C in PBST + 10% NGS + rat anti-BrdU (1:500; Accurate Chemical & Scientific Corp) + rabbit anti-GFP (1:500; Invitrogen/Fisher) using slow horizontal shaking.
13. Wash 8x in PBST, 20 min each.
14. Incubate O/N at 4°C in PBST + 10% NGS + rat Alexa Fluor 647 (1:500; Invitrogen/Fisher) + rabbit Alexa Fluor 488 (1:500; Invitrogen/Fisher).
15. Wash 6x in PBST, 10 min each.
16. Counterstain with 300 nM DAPI in PBST for 20 min.
17. Wash 3x in PBST, 5 min each.

7.9 DATA ACQUISITION, PROCESSING, AND ANALYSIS

The spatial parameters for imaging BrdU-stained neuromasts are the same as for live imaging. However, acquisition spectra should be adjusted to avoid spectral bleed-through and erroneous categorization of cell types.

To determine the spatial distribution of the distinct proliferating cell populations within a neuromast, obtain the positional data (X_n, Y_n) of $BrdU^+$ support cells, $BrdU^+$ hair cells (also *Sqet4*$^+$) and $BrdU^+$ mantle cells (also *sqet20*$^+$). These positional data will be used to compare spatial distributions and determine statistical significance.

Since a single neuromast, or the neuromasts of a single larva will not provide enough data for statistical robustness, the positional data of multiple neuromasts (approximately three) from different larvae (approximately six) must be overlaid and aligned to a common Cartesian plane. To achieve this, two parameters are needed: (1) the relative geometrical center of each neuromast and (2) a common X-axis.

1. To overlay the positional data from multiple imaged neuromasts, it is necessary to obtain the relative geometrical center of the neuromast (0,0). Acquire the geometrical center (X_c, Y_c) of each neuromast by drawing the contour of the neuromast using the Imaris surface tool (Fig. 4A, as described for the movement analysis).
2. To align every overlaid neuromast, it is necessary to set a common X-axis for every image. This standard X-axis is the horizontal line that can be traced from the left to the right interneuromast cells, which are directly in contact with the neuromast, also labeled with the *Tg(krt4:EGFP)*^{sqet20} transgene. To set this standard X-axis, acquire the nuclear image position of the left and right interneuromast cells (INC, Xnl_{INC}, Xnl_{INC}) for each imaged neuromast.
3. For each neuromast, calculate the relative position to the center of the neuromast of every BrdU+ cell (X, Y), and of the left and right interneuromast cells: (Xl_{INC}, Yl_{INC}) and (Xr_{INC}, Yr_{INC}). Every calculation should be done using spreadsheets.
4. Calculate the tilt angle of each neuromast (Fig. 4B) with respect to the horizontal axis using the relative position of the left and right interneuromast cells with the formula $\alpha = \mathrm{atan}((Yl_{INC} - Yr_{INC})/(Xl_{INC} - Xr))$.

5. To align each neuromast along a common horizontal axis (Xr, Yr) rotate the relative position (Fig. 4C) of every BrdU+ cell by calculating the rotated position using the formulas $Xr = (X * \cos(-\alpha)) - (Y * \sin(-\alpha))$, $Yr = (Y * \cos(-\alpha)) - (X * \sin(-\alpha))$.
6. To illustrate the relative position of cells, scatterplots can be easily generated in MS Excel (Fig. 4D–E).

7.10 STATISTICAL ANALYSES OF SPATIAL DISTRIBUTION

For statistical analyses, calculate the enrichment of $BrdU^+$ support cells in any of the quarters formed between the 45°, 135°, 225°, and 315° angles (Fig. 4D–E). These quadrants comprise the dorsoventral and anterior–posterior compartments previously described and which are characterized by differential gene expression (Wibowo et al., 2011; Romero-Carvajal et al., 2015).

7.10.1 Quadrant analysis

1. The enrichment of cells in any given quadrant can be determined using the angular position of each $BrdU^+$ nucleus. To address the density of angular positions in any given quadrant, perform a binomial analysis.
2. To illustrate the angular distribution of cells, generate rose diagrams using the gstat package of R (R Core Team, 2013).

7.10.2 Distance from center analysis

To calculate the distances of the $BrdU^+$ support and hair cell nuclei to the center of the neuromast, use the radii of their relative positions. The radii of the different cell types can then be compared using ANOVA.

CONCLUSIONS

The location of the sensory lateral line system in the skin makes the lateral line a powerful model to study cell behaviors during development and regeneration in vivo. The ability to image lateral line cell behavior at high resolution has been greatly facilitated by the generation of fluorescently labeled transgenic lines. In the future, the generation of endogenously tagged proteins using CRISPR technology will even further boost our ability to study cell biological processes in vivo.

ACKNOWLEDGMENTS

We thank the Stowers Institute for Medical Research (SIMR) Aquatics, Microscopy and Media Prep core facilities, and Mark Miller for help with graphical design. We would also like to thank Richard Alexander for developing the tools for the cell movement analysis and for critically reading the manuscript.

REFERENCES

Agarwala, S., Duquesne, S., Liu, K., Boehm, A., Grimm, L., Link, S. … Lecaudey, V. (2015). Amotl2a interacts with the Hippo effector Yap1 and the Wnt/beta-catenin effector Lef1 to control tissue size in zebrafish. *eLife, 4*.

Aman, A., Nguyen, M., & Piotrowski, T. (2011). Wnt/beta-catenin dependent cell proliferation underlies segmented lateral line morphogenesis. *Developmental Biology, 349*, 470–482.

Aman, A., & Piotrowski, T. (2008). Wnt/beta-catenin and Fgf signaling control collective cell migration by restricting chemokine receptor expression. *Developmental Cell, 15*, 749–761.

Aman, A., & Piotrowski, T. (2010). Cell migration during morphogenesis. *Developmental Biology, 341*, 20–33.

Ando, R., Hama, H., Yamamoto-Hino, M., Mizuno, H., & Miyawaki, A. (2002). An optical marker based on the UV-induced green-to-red photoconversion of a fluorescent protein. *Proceedings of the National Academy of Sciences of the United States of America, 99*, 12651–12656.

Ando, R., Mizuno, H., & Miyawaki, A. (2004). Regulated fast nucleocytoplasmic shuttling observed by reversible protein highlighting. *Science, 306*, 1370–1373.

Azuma, M., Toyama, R., Laver, E., & Dawid, I. B. (2006). Perturbation of rRNA synthesis in the bap28 mutation leads to apoptosis mediated by p53 in the zebrafish central nervous system. *Journal of Biological Chemistry, 281*, 13309–13316.

Breau, M. A., Wilkinson, D. G., & Xu, Q. (2013). A Hox gene controls lateral line cell migration by regulating chemokine receptor expression downstream of Wnt signaling. *Proceedings of the National Academy of Sciences of the United States of America, 110*, 16892–16897.

Brignull, H. R., Raible, D. W., & Stone, J. S. (2009). Feathers and fins: non-mammalian models for hair cell regeneration. *Brain Research, 1277*, 12–23.

Carmany-Rampey, A., & Moens, C. B. (2006). Modern mosaic analysis in the zebrafish. *Methods, 39*, 228–238.

Carney, T. J., Dutton, K. A., Greenhill, E., Delfino-Machin, M., Dufourcq, P., Blader, P., & Kelsh, R. N. (2006). A direct role for Sox10 in specification of neural crest-derived sensory neurons. *Development, 133*, 4619–4630.

Chazotte, B. (2011). Labeling nuclear DNA using DAPI. *Cold Spring Harbor Protocols, 2011*. pdb.prot5556.

Chen, Y. Y., Harris, M. P., Levesque, M. P., Nusslein-Volhard, C., & Sonawane, M. (2012). Heterogeneity across the dorso-ventral axis in zebrafish EVL is regulated by a novel module consisting of sox, snail1a and max genes. *Mechanisms of Development, 129*, 13–23.

Chitnis, A. B., Nogare, D. D., & Matsuda, M. (2012). Building the posterior lateral line system in zebrafish. *Developmental Neurobiology, 72*, 234–255.

Cooper, M. S., D'Amico, L. A., & Henry, C. A. (1999). Confocal microscopic analysis of morphogenetic movements. *Methods in Cell Biology, 59*, 179–204.

Cooper, M. S., Szeto, D. P., Sommers-Herivel, G., Topczewski, J., Solnica-Krezel, L., Kang, H. C. … Kimelman, D. (2005). Visualizing morphogenesis in transgenic zebrafish embryos using BODIPY TR methyl ester dye as a vital counterstain for GFP. *Developmental Dynamics: An Official Publication of the American Association of Anatomists, 232*, 359–368.

Cruz, I. A., Kappedal, R., Mackenzie, S. M., Hailey, D. W., Hoffman, T. L., Schilling, T. F., & Raible, D. W. (2015). Robust regeneration of adult zebrafish lateral line hair cells reflects continued precursor pool maintenance. *Developmental Biology, 402*, 229–238.

Dalle Nogare, D., Somers, K., Rao, S., Matsuda, M., Reichman-Fried, M., Raz, E., & Chitnis, A. B. (2014). Leading and trailing cells cooperate in collective migration of the zebrafish posterior lateral line primordium. *Development, 141*, 3188–3196.

Dambly-Chaudiere, C., Sapede, D., Soubiran, F., Decorde, K., Gompel, N., & Ghysen, A. (2003). The lateral line of zebrafish: a model system for the analysis of morphogenesis and neural development in vertebrates. *Biology of the Cell/Under the Auspices of the European Cell Biology Organization, 95*, 579–587.

David, N. B., Sapede, D., Saint-Etienne, L., Thisse, C., Thisse, B., Dambly-Chaudiere, C. … Ghysen, A. (2002). Molecular basis of cell migration in the fish lateral line: role of the chemokine receptor CXCR4 and of its ligand, SDF1. *Proceedings of the National Academy of Sciences of the United States of America, 99*, 16297–16302.

Diotel, N., Do Rego, J. L., Anglade, I., Vaillant, C., Pellegrini, E., Vaudry, H., & Kah, O. (2011). The brain of teleost fish, a source, and a target of sexual steroids. *Frontiers in Neuroscience, 5*, 137.

Distel, M., & Koster, R. W. (2007). In vivo time-lapse imaging of zebrafish embryonic development. *CSH Protoc 2007*. pdb prot4816.

Dolez, M., Nicolas, J. F., & Hirsinger, E. (2011). Laminins, via heparan sulfate proteoglycans, participate in zebrafish myotome morphogenesis by modulating the pattern of Bmp responsiveness. *Development, 138*, 97–106.

Dona, E., Barry, J. D., Valentin, G., Quirin, C., Khmelinskii, A., Kunze, A. … Gilmour, D. (2013). Directional tissue migration through a self-generated chemokine gradient. *Nature, 503*, 285–289.

Ernst, S., Liu, K., Agarwala, S., Moratscheck, N., Avci, M. E., Dalle Nogare, D. … Lecaudey, V. (2012). Shroom3 is required downstream of FGF signalling to mediate proneuromast assembly in zebrafish. *Development, 139*, 4571–4581.

Faucherre, A., Pujol-Marti, J., Kawakami, K., & Lopez-Schier, H. (2009). Afferent neurons of the zebrafish lateral line are strict selectors of hair-cell orientation. *PLoS One, 4*, e4477.

Fritzsch, B., & Straka, H. (2014). Evolution of vertebrate mechanosensory hair cells and inner ears: toward identifying stimuli that select mutation driven altered morphologies. *Journal of Comparative Physiology A, Neuroethology, Sensory, Neural, and Behavioral Physiology, 200*, 5–18.

Furness, D. N. (2015). Molecular basis of hair cell loss. *Cell and Tissue Research, 361*, 387–399.

Ghysen, A., & Dambly-Chaudiere, C. (2004). Development of the zebrafish lateral line. *Current Opinion in Neurobiology, 14*, 67–73.

Ghysen, A., & Dambly-Chaudiere, C. (2007). The lateral line microcosmos. *Genes and Development, 21*, 2118–2130.

Gilmour, D., Knaut, H., Maischein, H. M., & Nusslein-Volhard, C. (2004). Towing of sensory axons by their migrating target cells in vivo. *Nature Neuroscience, 7*, 491–492.

Gilmour, D. T., Maischein, H. M., & Nusslein-Volhard, C. (2002). Migration and function of a glial subtype in the vertebrate peripheral nervous system. *Neuron, 34*, 577–588.

Goodrich, L. V. (2005). Hear, hear for the zebrafish. *Neuron, 45*, 3–5.

Grant, K. A., Raible, D. W., & Piotrowski, T. (2005). Regulation of latent sensory hair cell precursors by glia in the zebrafish lateral line. *Neuron, 45*, 69–80.

Gurskaya, N. G., Verkhusha, V. V., Shcheglov, A. S., Staroverov, D. B., Chepurnykh, T. V., Fradkov, A. F. … Lukyanov, K. A. (2006). Engineering of a monomeric green-to-red photoactivatable fluorescent protein induced by blue light. *Nature Biotechnology, 24*, 461–465.

Haas, P., & Gilmour, D. (2006). Chemokine signaling mediates self-organizing tissue migration in the zebrafish lateral line. *Developmental Cell, 10*, 673–680.

Harding, M. J., McGraw, H. F., & Nechiporuk, A. (2014). The roles and regulation of multicellular rosette structures during morphogenesis. *Development, 141*, 2549–2558.

Harding, M. J., & Nechiporuk, A. V. (2012). Fgfr-Ras-MAPK signaling is required for apical constriction via apical positioning of Rho-associated kinase during mechanosensory organ formation. *Development, 139*, 3130–3135.

Harris, J. A., Cheng, A. G., Cunningham, L. L., MacDonald, G., Raible, D. W., & Rubel, E. W. (2003). Neomycin-induced hair cell death and rapid regeneration in the lateral line of zebrafish (*Danio rerio*). *Journal of the Association for Research in Otolaryngology: JARO, 4*, 219–234.

Hatta, K., Tsujii, H., & Omura, T. (2006). Cell tracking using a photoconvertible fluorescent protein. *Nature Protocols, 1*, 960–967.

Hava, D., Forster, U., Matsuda, M., Cui, S., Link, B. A., Eichhorst, J. … Abdelilah-Seyfried, S. (2009). Apical membrane maturation and cellular rosette formation during morphogenesis of the zebrafish lateral line. *Journal of Cell Science, 122*, 687–695.

Hernandez, P. P., Olivari, F. A., Sarrazin, A. F., Sandoval, P. C., & Allende, M. L. (2007). Regeneration in zebrafish lateral line neuromasts: expression of the neural progenitor cell marker sox2 and proliferation-dependent and -independent mechanisms of hair cell renewal. *Developmental Neurobiology, 67*, 637–654.

Hogan, B. M., Verkade, H., Lieschke, G. J., & Heath, J. K. (2008). Manipulation of gene expression during zebrafish embryonic development using transient approaches. *Methods in Molecular Biology, 469*, 273–300.

Itoh, M., & Chitnis, A. B. (2001). Expression of proneural and neurogenic genes in the zebrafish lateral line primordium correlates with selection of hair cell fate in neuromasts. *Mechanisms of Development, 102*, 263–266.

Itoh, M., Kim, C. H., Palardy, G., Oda, T., Jiang, Y. J., Maust, D. … Chitnis, A. B. (2003). Mind bomb is a ubiquitin ligase that is essential for efficient activation of Notch signaling by Delta. *Developmental Cell, 4*, 67–82.

Jiang, L., Romero-Carvajal, A., Haug, J. S., Seidel, C. W., & Piotrowski, T. (2014). Gene-expression analysis of hair cell regeneration in the zebrafish lateral line. *Proceedings of the National Academy of Sciences of the United States of America, 111*, E1383–E1392.

Jonkman, J., & Brown, C. M. (2015). Any way you slice it-a comparison of confocal microscopy techniques. *Journal of Biomolecular Techniques: JBT, 26*, 54–65.

Jurynec, M. J., Xia, R., Mackrill, J. J., Gunther, D., Crawford, T., Flanigan, K. M. … Grunwald, D. J. (2008). Selenoprotein N is required for ryanodine receptor calcium release channel activity in human and zebrafish muscle. *Proceedings of the National Academy of Sciences of the United States of America, 105*, 12485–12490.

Kamei, M., & Weinstein, B. M. (2005). Long-term time-lapse fluorescence imaging of developing zebrafish. *Zebrafish, 2*(2), 113–123.

Kaufmann, A., et al. (2012). Multilayer mounting enables long-term imaging of zebrafish development in a light sheet microscope. *Development, 139*(17), 3242–3247.

Kemp, H. A., Carmany-Rampey, A., & Moens, C. (2009). Generating chimeric zebrafish embryos by transplantation. *Journal of Visualized Experiments: JoVE, 29*.

Kerstetter, A. E., Azodi, E., Marrs, J. A., & Liu, Q. (2004). Cadherin-2 function in the cranial ganglia and lateral line system of developing zebrafish. *Developmental Dynamics: An Official Publication of the American Association of Anatomists, 230*, 137–143.

Kimmel, C. B., Ballard, W. W., Kimmel, S. R., Ullmann, B., & Schilling, T. F. (1995). Stages of embryonic development of the zebrafish. *Developmental Dynamics: An Official Publication of the American Association of Anatomists, 203*, 253–310.

Kindt, K. S., Finch, G., & Nicolson, T. (2012). Kinocilia mediate mechanosensitivity in developing zebrafish hair cells. *Developmental Cell, 23*, 329–341.

Kollmar, R., Nakamura, S. K., Kappler, J. A., & Hudspeth, A. J. (2001). Expression and phylogeny of claudins in vertebrate primordia. *Proceedings of the National Academy of Sciences of the United States of America, 98*, 10196–10201.

Kozlowski, D. J., Murakami, T., Ho, R. K., & Weinberg, E. S. (1997). Regional cell movement and tissue patterning in the zebrafish embryo revealed by fate mapping with caged fluorescein. *Biochemistry and Cell Biology = Biochimie et biologie cellulaire, 75*, 551–562.

Lauter, G., Soll, I., & Hauptmann, G. (2014). Sensitive whole-mount fluorescent in situ hybridization in zebrafish using enhanced tyramide signal amplification. *Methods in Molecular Biology, 1082*, 175–185.

Lecaudey, V., Cakan-Akdogan, G., Norton, W. H., & Gilmour, D. (2008). Dynamic Fgf signaling couples morphogenesis and migration in the zebrafish lateral line primordium. *Development, 135*, 2695–2705.

Li, Q., Shirabe, K., & Kuwada, J. Y. (2004). Chemokine signaling regulates sensory cell migration in zebrafish. *Developmental Biology, 269*, 123–136.

Li, P., White, R. M., & Zon, L. I. (2011). Transplantation in zebrafish. *Methods in Cell Biology, 105*, 403–417.

Lombardo, V. A., Sporbert, A., & Abdelilah-Seyfried, S. (2012). Cell tracking using photoconvertible proteins during zebrafish development. *Journal of Visualized Experiments: JoVE, 28*.

Lopez-Schier, H., & Hudspeth, A. J. (2005). Supernumerary neuromasts in the posterior lateral line of zebrafish lacking peripheral glia. *Proceedings of the National Academy of Sciences of the United States of America, 102*, 1496–1501.

Lopez-Schier, H., & Hudspeth, A. J. (2006). A two-step mechanism underlies the planar polarization of regenerating sensory hair cells. *Proceedings of the National Academy of Sciences of the United States of America, 103*, 18615–18620.

Lopez-Schier, H., Starr, C. J., Kappler, J. A., Kollmar, R., & Hudspeth, A. J. (2004). Directional cell migration establishes the axes of planar polarity in the posterior lateral-line organ of the zebrafish. *Developmental Cell, 7*, 401–412.

Lush, M. E., & Piotrowski, T. (2014a). ErbB expressing Schwann cells control lateral line progenitor cells via non-cell-autonomous regulation of Wnt/beta-catenin. *eLife, 3*, e01832.

Lush, M. E., & Piotrowski, T. (2014b). Sensory hair cell regeneration in the zebrafish lateral line. *Developmental Dynamics: An Official Publication of the American Association of Anatomists, 243*, 1187–1202.

Lyons, D. A., Pogoda, H. M., Voas, M. G., Woods, I. G., Diamond, B., Nix, R. … Talbot, W. S. (2005). erbb3 and erbb2 are essential for Schwann cell migration and myelination in zebrafish. *Current Biology: CB, 15*, 513–524.

Ma, E. Y., Rubel, E. W., & Raible, D. W. (2008). Notch signaling regulates the extent of hair cell regeneration in the zebrafish lateral line. *The Journal of Neuroscience: The Official Journal of the Society for Neuroscience, 28*, 2261–2273.

Mackenzie, S. M., & Raible, D. W. (2012). Proliferative regeneration of zebrafish lateral line hair cells after different ototoxic insults. *PLoS One, 7*, e47257.

Malicki, J., Jo, H., & Pujic, Z. (2003). Zebrafish N-cadherin, encoded by the glass onion locus, plays an essential role in retinal patterning. *Developmental Biology, 259*, 95−108.

Matsuda, M., & Chitnis, A. B. (2010). Atoh1a expression must be restricted by Notch signaling for effective morphogenesis of the posterior lateral line primordium in zebrafish. *Development, 137*, 3477−3487.

Matsuda, M., Nogare, D. D., Somers, K., Martin, K., Wang, C., & Chitnis, A. B. (2013). Lef1 regulates Dusp6 to influence neuromast formation and spacing in the zebrafish posterior lateral line primordium. *Development, 140*, 2387−2397.

McGraw, H. F., Culbertson, M. D., & Nechiporuk, A. V. (2014). Kremen1 restricts Dkk activity during posterior lateral line development in zebrafish. *Development, 141*, 3212−3221.

McGraw, H. F., Drerup, C. M., Culbertson, M. D., Linbo, T., Raible, D. W., & Nechiporuk, A. V. (2011). Lef1 is required for progenitor cell identity in the zebrafish lateral line primordium. *Development, 138*, 3921−3930.

Metcalfe, W. K. (1985). Sensory neuron growth cones comigrate with posterior lateral line primordial cells in zebrafish. *The Journal of Comparative Neurology, 238*, 218−224.

Metcalfe, W. K., Kimmel, C. B., & Schabtach, E. (1985). Anatomy of the posterior lateral line system in young larvae of the zebrafish. *The Journal of Comparative Neurology, 233*, 377−389.

Meyers, J. R., Planamento, J., Ebrom, P., Krulewitz, N., Wade, E., & Pownall, M. E. (2013). Sulf1 modulates BMP signaling and is required for somite morphogenesis and development of the horizontal myoseptum. *Developmental Biology, 378*, 107−121.

Mirkovic, I., Pylawka, S., & Hudspeth, A. J. (2012). Rearrangements between differentiating hair cells coordinate planar polarity and the establishment of mirror symmetry in lateral-line neuromasts. *Biology Open, 1*, 498−505.

Moens, C. (2008a). Whole mount RNA in situ hybridization on zebrafish embryos: hybridization. *CSH Protocols, 2008*. pdb prot5037.

Moens, C. (2008b). Whole mount RNA in situ hybridization on zebrafish embryos: probe synthesis. *CSH Protocols, 2008*. pdb prot5036.

Nagayoshi, S., Hayashi, E., Abe, G., Osato, N., Asakawa, K., Urasaki, A. … Kawakami, K. (2008). Insertional mutagenesis by the Tol2 transposon-mediated enhancer trap approach generated mutations in two developmental genes: tcf7 and synembryn-like. *Development, 135*, 159−169.

Nagiel, A., Andor-Ardo, D., & Hudspeth, A. J. (2008). Specificity of afferent synapses onto plane-polarized hair cells in the posterior lateral line of the zebrafish. *The Journal of Neuroscience: The Official Journal of the Society for Neuroscience, 28*, 8442−8453.

Nechiporuk, A., & Raible, D. W. (2008). FGF-dependent mechanosensory organ patterning in zebrafish. *Science, 320*, 1774−1777.

Nikaido, M., Kawakami, A., Sawada, A., Furutani-Seiki, M., Takeda, H., & Araki, K. (2002). Tbx24, encoding a T-box protein, is mutated in the zebrafish somite-segmentation mutant fused somites. *Nature Genetics, 31*, 195−199.

Norton, W. H., Ledin, J., Grandel, H., & Neumann, C. J. (2005). HSPG synthesis by zebrafish Ext2 and Extl3 is required for Fgf10 signalling during limb development. *Development, 132*, 4963−4973.

Ou, H. C., Raible, D. W., & Rubel, E. W. (2007). Cisplatin-induced hair cell loss in zebrafish (*Danio rerio*) lateral line. *Hearing Research, 233*, 46−53.

Pan, Y. A., Freundlich, T., Weissman, T. A., Schoppik, D., Wang, X. C., Zimmerman, S. … Schier, A. F. (2013). Zebrabow: multispectral cell labeling for cell tracing and lineage analysis in zebrafish. *Development, 140*, 2835–2846.

Parinov, S., Kondrichin, I., Korzh, V., & Emelyanov, A. (2004). Tol2 transposon-mediated enhancer trap to identify developmentally regulated zebrafish genes in vivo. *Developmental Dynamics: An Official Publication of the American Association of Anatomists, 231*, 449–459.

Parsons, M. J., Pisharath, H., Yusuff, S., Moore, J. C., Siekmann, A. F., Lawson, N., & Leach, S. D. (2009). Notch-responsive cells initiate the secondary transition in larval zebrafish pancreas. *Mechanisms of Development, 126*, 898–912.

Perlin, J. R., Lush, M. E., Stephens, W. Z., Piotrowski, T., & Talbot, W. S. (2011). Neuronal Neuregulin 1 type III directs Schwann cell migration. *Development, 138*, 4639–4648.

Pezeron, G., Anselme, I., Laplante, M., Ellingsen, S., Becker, T. S., Rosa, F. M. … Ghislain, J. (2006). Duplicate sfrp1 genes in zebrafish: sfrp1a is dynamically expressed in the developing central nervous system, gut and lateral line. *Gene Expression Patterns: GEP, 6*, 835–842.

Pinto-Teixeira, F., Muzzopappa, M., Swoger, J., Mineo, A., Sharpe, J., & Lopez-Schier, H. (2013). Intravital imaging of hair-cell development and regeneration in the zebrafish. *Frontiers in Neuroanatomy, 7*, 33.

Piotrowski, T., & Baker, C. V. (2014). The development of lateral line placodes: taking a broader view. *Developmental Biology, 389*, 68–81.

Renaud, O., et al. (2011). Studying cell behavior in whole zebrafish embryos by confocal live imaging: application to hematopoietic stem cells. *Nat Protoc, 6*(12), 1897–1904.

Revenu, C., Streichan, S., Dona, E., Lecaudey, V., Hufnagel, L., & Gilmour, D. (2014). Quantitative cell polarity imaging defines leader-to-follower transitions during collective migration and the key role of microtubule-dependent adherens junction formation. *Development, 141*, 1282–1291.

Rombough, P. J. (2007). Ontogenetic changes in the toxicity and efficacy of the anaesthetic MS222 (tricaine methanesulfonate) in zebrafish (Danio rerio) larvae. *Comp Biochem Physiol A Mol Integr Physiol, 148*(2), 463–469.

Romero-Carvajal, A., Navajas Acedo, J., Jiang, L., Kozlovskaja-Gumbriene, A., Alexander, R., Li, H., & Piotrowski, T. (2015). Regeneration of sensory hair cells requires localized interactions between the Notch and Wnt pathways. *Developmental Cell, 34*, 267–282.

Santos, F., MacDonald, G., Rubel, E. W., & Raible, D. W. (2006). Lateral line hair cell maturation is a determinant of aminoglycoside susceptibility in zebrafish (*Danio rerio*). *Hearing Research, 213*, 25–33.

Sato, T., Takahoko, M., & Okamoto, H. (2006). HuC: Kaede, a useful tool to label neural morphologies in networks in vivo. *Genesis, 44*, 136–142.

Schuster, K., & Ghysen, A. (2013). Labeling defined cells or subsets of cells in zebrafish by Kaede photoconversion. *Cold Spring Harbor Protocols, 2013*.

Shimizu, N., Kawakami, K., & Ishitani, T. (2012). Visualization and exploration of Tcf/Lef function using a highly responsive Wnt/beta-catenin signaling-reporter transgenic zebrafish. *Developmental Biology, 370*, 71–85.

Shin, J., Chen, J., & Solnica-Krezel, L. (2014). Efficient homologous recombination-mediated genome engineering in zebrafish using TALE nucleases. *Development, 141*, 3807–3818.

Shoji, W., Yee, C. S., & Kuwada, J. Y. (1998). Zebrafish semaphorin Z1a collapses specific growth cones and alters their pathway in vivo. *Development, 125*, 1275–1283.

Sienknecht, U. J., Koppl, C., & Fritzsch, B. (2014). Evolution and development of hair cell polarity and efferent function in the inner ear. *Brain, Behavior and Evolution, 83*, 150–161.

Steiner, A. B., Kim, T., Cabot, V., & Hudspeth, A. J. (2014). Dynamic gene expression by putative hair-cell progenitors during regeneration in the zebrafish lateral line. *Proceedings of the National Academy of Sciences of the United States of America, 111*, E1393–E1401.

Subramanian, A., & Schilling, T. F. (2014). Thrombospondin-4 controls matrix assembly during development and repair of myotendinous junctions. *eLife, 3*.

Thisse, C., & Thisse, B. (2008). High-resolution in situ hybridization to whole-mount zebrafish embryos. *Nature Protocols, 3*, 59–69.

Thisse, B., & Thisse, C. (2014). In situ hybridization on whole-mount zebrafish embryos and young larvae. *Methods in Molecular Biology, 1211*, 53–67.

Thomas, E. D., Cruz, I. A., Hailey, D. W., & Raible, D. W. (2015). There and back again: development and regeneration of the zebrafish lateral line system. *Wiley Interdisciplinary Reviews Developmental Biology, 4*, 1–16.

Tsutsui, H., Karasawa, S., Shimizu, H., Nukina, N., & Miyawaki, A. (2005). Semi-rational engineering of a coral fluorescent protein into an efficient highlighter. *EMBO Reports, 6*, 233–238.

Valdivia, L. E., Young, R. M., Hawkins, T. A., Stickney, H. L., Cavodeassi, F., Schwarz, Q. … Wilson, S. W. (2011). Lef1-dependent Wnt/beta-catenin signalling drives the proliferative engine that maintains tissue homeostasis during lateral line development. *Development, 138*, 3931–3941.

Valentin, G., Haas, P., & Gilmour, D. (2007). The chemokine SDF1a coordinates tissue migration through the spatially restricted activation of Cxcr7 and Cxcr4b. *Current Biology: CB, 17*, 1026–1031.

Venero Galanternik, M., Kramer, K. L., & Piotrowski, T. (2015). Heparan sulfate proteoglycans regulate Fgf signaling and cell polarity during collective cell migration. *Cell Reports, 10*.

Venkiteswaran, G., Lewellis, S. W., Wang, J., Reynolds, E., Nicholson, C., & Knaut, H. (2013). Generation and dynamics of an endogenous, self-generated signaling gradient across a migrating tissue. *Cell, 155*, 674–687.

Villablanca, E. J., Renucci, A., Sapede, D., Lec, V., Soubiran, F., Sandoval, P. C. … Allende, M. L. (2006). Control of cell migration in the zebrafish lateral line: implication of the gene "tumour-associated calcium signal transducer," tacstd. *Developmental Dynamics: An Official Publication of the American Association of Anatomists, 235*, 1578–1588.

Wada, H., Ghysen, A., Asakawa, K., Abe, G., Ishitani, T., & Kawakami, K. (2013). Wnt/Dkk negative feedback regulates sensory organ size in zebrafish. *Current Biology: CB, 23*, 1559–1565.

Wada, H., Ghysen, A., Satou, C., Higashijima, S., Kawakami, K., Hamaguchi, S., & Sakaizumi, M. (2010). Dermal morphogenesis controls lateral line patterning during postembryonic development of teleost fish. *Developmental Biology, 340*, 583–594.

Welten, M. C., de Haan, S. B., van den Boogert, N., Noordermeer, J. N., Lamers, G. E., Spaink, H. P. … Verbeek, F. J. (2006). ZebraFISH: fluorescent in situ hybridization protocol and three-dimensional imaging of gene expression patterns. *Zebrafish, 3*, 465–476.

Whitfield, T. T. (2005). Lateral line: precocious phenotypes and planar polarity. *Current Biology: CB, 15*, R67–R70.

Wibowo, I., Pinto-Teixeira, F., Satou, C., Higashijima, S., & Lopez-Schier, H. (2011). Compartmentalized Notch signaling sustains epithelial mirror symmetry. *Development, 138*, 1143–1152.

Xiao, T., Roeser, T., Staub, W., & Baier, H. (2005). A GFP-based genetic screen reveals mutations that disrupt the architecture of the zebrafish retinotectal projection. *Development, 132*, 2955–2967.

Xing, C., Gong, B., Xue, Y., Han, Y., Wang, Y., Meng, A., & Jia, S. (2015). TGFbeta1a regulates zebrafish posterior lateral line formation via Smad5 mediated pathway. *Journal of Molecular Cell Biology, 7*, 48–61.

Yeo, S. Y., Kim, M., Kim, H. S., Huh, T. L., & Chitnis, A. B. (2007). Fluorescent protein expression driven by her4 regulatory elements reveals the spatiotemporal pattern of Notch signaling in the nervous system of zebrafish embryos. *Developmental Biology, 301*, 555–567.